

**MODELLING AND STRUCTURAL ANALYSIS OF THE BALL-ON-SPHERE
SYSTEM USING BOND GRAPH TECHNIQUE**

BY

ABDULMUMINI YESUFU

**DEPARTMENT OF ELECTRICAL AND COMPUTER ENGINEERING,
FACULTY OF ENGINEERING,
AHMADU BELLO UNIVERSITY,
ZARIA, NIGERIA.**

JANUARY, 2017

**MODELLING AND STRUCTURAL ANALYSIS OF THE BALL-ON-SPHERE
SYSTEM USING BOND GRAPH TECHNIQUE**

BY

**ABDULMUMINI YESUFU, B.ENG (UNILORIN) 2010
M.SC/ENG/22675/2012-2013
mumincome2008@yahoo.com**

**A DISSERTATION SUBMITTED TO THE SCHOOL OF POST GRADUATE
STUDIES AHMADU BELLO UNIVERSITY, ZARIA IN PARTIAL
FULFILLMENT OF THE REQUIREMENTS FOR THE AWARD OF A
MASTER OF SCIENCE (M.SC) DEGREE IN CONTROL ENGINEERING**

**DEPARTMENT OF ELECTRICAL AND COMPUTER ENGINEERING,
FACULTY OF ENGINEERING,
AHMADU BELLO UNIVERSITY,
ZARIA, NIGERIA.**

JANUARY, 2017

DECLARATION

I YESUFU Abdulmumini, hereby declare that the work in this Dissertation entitled “Modelling and Structural Analysis of Ball-on-Sphere System using Bond Graph Technique” has been carried out by me in the Department of Electrical and Computer Engineering. The information derived from literature has been duly acknowledged in the text and a list of references provided. No part of this dissertation was previously presented for another degree or diploma at this or any other institution.

YESUFU Abdulmumini
Name of Student

Signature

Date

CERTIFICATION

This Dissertation entitled “MODELLING AND STRUCTURAL ANALYSIS OF THE BALL-ON-SPHERE SYSTEM USING BOND GRAPH TECHNIQUE” by Abdulmumini YESUFU meets the regulations governing the award of degree of Master of Science (MSc) in Control Engineering of the Ahmadu Bello University, and is approved for its contribution to knowledge and literary presentation.

(Prof. M. B. Mu'azu)

Chairman, Supervisory Committee	(Signature)	Date
---------------------------------	-------------	------

(Dr. A.D. Usman)

Member, Supervisory Committee	(Signature)	Date
-------------------------------	-------------	------

(Dr. Y. Jibril)

Head of Department	(Signature)	Date
--------------------	-------------	------

(Prof. S.Z. Abubakar)

Dean, School of Postgraduate Studies	(Signature)	Date
--------------------------------------	-------------	------

DEDICATION

This dissertation work is humbly dedicated to God Almighty and my parents.

ACKNOWLEDGEMENT

I am indeed grateful to Almighty Allah for His Infinite Blessings and Guidance towards the successful completion of this work.

I express my utmost gratitude to my supervisor and the chairman of my supervisory committee, Prof. M. B. Mu'azu, for his time, immense contributions and valuable guidance towards the success of this work. Indeed, the completion of this work could not have been possible without your consistent participation and assistance. I am proud to have you as my supervisor. You helped me to shape the research problem and provided valuable insight on the solution to the problem. Thank you very much Prof. My thanks also goes to my co-supervisor Dr. A.D. Usman for his valuable input and constant encouragement throughout the stages of the work. I really appreciate the training I received from you. My deep appreciation goes to the students of the Control & Computer Research Group for their valuable contributions, suggestion and constructive criticism during the discussion stages of my work.

I acknowledge and appreciate all the lecturers of Electrical and Computer Engineering, Ahmadu Bello University for their immense contributions towards the success of this work. My sincere appreciation also goes to Mr. Abdullahi Tukur for his administrative support towards the completion of the work.

My special thanks go to Ovie Ese, Suleiman Hussein, Kabir Rashid, Salawudeen A. Tijjani, Olaniyan AbdulRahman, Arafat Ndubisi, Valentine Ikpo, Daniel Aliyu and Obute Simon for their valuable contributions and support toward the success of this work. I am indeed grateful to you guys, your handsome reward is with God. I am very much thankful to all my course mates, especially Ndubisi, Busayo and Abubakar for your encouragement and persistence. God will reward you all.

I am really indebted to my parents Alhaji M.O Yesufu and Mrs. Abibetu Yesufu for your continuous love and support. Your kind advice and understanding will always be appreciated. Thank you very much. My gratitude also goes to my siblings and the entire member of my family. I really thank you all for your love and support.

Abdulumini YESUFU
January, 2017

ABSTRACT

This research is aimed at the modelling and structural analysis of the ball-on-sphere system using bond graph technique. To achieve the bond graph model of the ball-on-sphere system, the various subsystems, storage elements, junction structures, transformer elements with appropriate causality assignments and energy exchange that make up the ball-on-sphere system were identified and modelled. The developed bond graph model of the ball-on-sphere system overcame the computational complexities involved using Euler-Lagrange modelling technique which is prone to modelling errors. 20-Sim software was used to validate the developed bond graph model. In the developed bond graph model considering the effect of friction, the time of angular position response of the ball (β) achieved was 0.5253s while in the system model without frictional effect, time of 0.5408s was achieved for the angular position response of the ball (β). This shows 2.9% improvement of the angular position response of the ball considering frictional effect in the developed bond graph model. It was established from the structural analysis that the developed model of the ball-on-sphere system was controllable and observable. It was also determined from the structural analysis that the system was invertible and input-output decouplable.

TABLE OF CONTENTS

TITLE PAGE	I
DECLARATION	II
CERTIFICATION	III
DEDICATION	IV
ACKNOWLEDGEMENT	V
ABSTRACT	VII
LIST OF APPENDICES	XI
LIST OF FIGURES	XII
LIST OF TABLES	XIVV
LIST OF ABBREVIATIONS	XV

CHAPTER ONE: INTRODUCTION

1.1 BACKGROUND	1
1.2 MOTIVATION	2
1.3 STATEMENT OF PROBLEM	3
1.4 AIM AND OBJECTIVES	4
1.5 DISSERTATION ORGANIZATION	4

CHAPTER TWO :LITERATURE REVIEW

2.1 INTRODUCTION	6
2.2 REVIEW OF FUNDAMENTAL CONCEPTS	6
2.2.1 Ball-on-Sphere System	6

2.2.2 Mathematical Model of Ball-on-Sphere System	6
2.2.3 Bond Graph Modelling Technique	9
2.2.4 Causality Concept	12
2.2.5 20-Sim Software	17
2.2.6 Structural Analysis Concept	19
2.3 REVIEW OF SIMILAR WORKS	25

CHAPTER THREE :METHODS AND MATERIALS

3.1 INTRODUCTION	32
3.2 METHODOLOGY	32
3.3 BALL-ON-SPHERE MODELLING	33
3.3.1 Bond Graph Modelling of Ball-on-Sphere System	33
3.3.2 Ball-on-Sphere System Causalities Assignment	34
3.3.3 Ball-on-Sphere System Equations Derivation	35
3.3.4 Ball-on-Sphere Bond Graph Subcomponents	44
3.3.5 Simulink Model of the Ball-on-Sphere System	46
3.4 20-SIM VALIDATION OF BOND-ON-SPHERE SYSTEM MODEL	49
3.5 STRUCTURAL ANALYSIS OF THE BALL-ON-SPHERE SYSTEM	50
3.5.1 Ball-on-Sphere System Structural Controllability Analysis	50
3.5.2 Ball-on-Sphere System Structural Observability Analysis	51
3.5.3 Ball-on-Sphere System Inverse Model Analysis	53
3.5.4 Ball-on-Sphere System Input-Output Decoupling Analysis	55
3.6 STATE SPACE GENERATION OF THE BALL-ON-SPHERE MODEL	55
3.7 MATRIX APPROACH OF INVERTIBILITY AND DECOUPLING OF BALL-ON-SPHERE SYSTEM	58

CHAPTER FOUR: RESULTS AND DISCUSSION

4.1 INTRODUCTION	61
4.2 BALL-ON-SPHERE SYSTEM MODEL	61
4.2.1 Bond Graph Model of Ball-on-Sphere System	61
4.2.2 Bond Graph Causal Model of Ball-on-Sphere System	62
4.2.3 Mathematical Model of Ball-on-Sphere System	64
4.3 20-SIM VALIDATION OF BALL-ON-SPHERE SYSTEM MODEL	65
4.4 STRUCTURAL ANALYSIS OF THE BALL-ON-SPHERE SYSTEM	66
4.4.1 Ball-on-Sphere System Structural Controllability Analysis	66
4.4.2 Ball-on-Sphere System Structural Observability Analysis	68
4.4.3 Ball-on-Sphere System Bond Graph Inverse Model	70
4.4.4 Ball-on-Sphere System Input-Output Decoupling Analysis	71
4.5 NUMERICAL APPROACH TO THE BALL-ON-SPHERE SYSTEM ANALYSES	73
4.6 RESULTS OF BALL-ON-SPHERE MODEL ANALYSIS	74
CHAPTER FIVE: CONCLUSION AND RECOMMENDATION	
5.1 SUMMARY	76
5.2 CONCLUSION	76
5.3 LIMITATION	77
5.4 SIGNIFICANT CONTRIBUTIONS	77
5.5 RECOMMENDATIONS FOR FURTHER WORK	78
REFERENCES	79

LIST OF APPENDICES

APPENDIX A	83
BALL-ON-SPHERE SYSTEM CONTROLLABILITY AND OBSERVABILITY ANALYSIS	83
APPENDIX B	85
BALL-ON-SPHERE MODEL ANALYSIS	85

LIST OF FIGURES

Figure 1.1: Ball on a Sphere System	1
Figure 2.1: Ball-on-Sphere System	7
Figure 2.2: Ball-on-Sphere System in the x- Direction	9
Figure 2.3: Schematic Diagram of Energy	11
Figure 2.4a: Capacitance (C) Causality Integral Configuration	13
Figure 2.4b: Capacitance (C) Differential Configuration	13
Figure 2.5a: Inertance (I) Causality Integral Configuration	14
Figure 2.5b: Inertance (I) Causality Differential Configuration	14
Figure 2.6a: Resistance (R) Causality Integral Configuration	14
Figure 2.6b: Resistance (R) Differential Configuration	14
Figure 2.7: 20-Sim Graphical User Interface	18
Figure 2.8: Bi-causal Bond Graph for Two Physical Subsystems (S1, S2)	22
Figure 2.9: General representation of a Bond Graph Direct Model	23
Figure 2.10: General Representation of a Bond Graph Inverse Model	23
Figure 3.1: Ball and Wheel System in x-axis	33
Figure 3.2: Bond Graph Structure of Ball-on-Sphere System	36
Figure 3.3: 20-Sim Model Equations for Ball-on-Sphere System	42
Figure 3.4: Sphere Dynamic Information	44
Figure 3.5: Rotational and Translational Ball Dynamics	44
Figure 3.6: Simulink Model of Ball-on-Sphere System	49
Figure 3.7: Causal Path of Source and Storage elements for Controlability Analysis	51
Figure 3.8: Derivative Storage Elements for Controllability Analysis	51
Figure 3.9: Causal Path Connecting Storage Elements and Detector for Observability Analysis	52

Figure 3.10: Derivative Storage Elements for Observability Analysis	53
Figure 3.11: Disjoints Input-Output Causal Path for Invertibility Analysis	54
Figure 3.12: Bicausality for Ball-on-Sphere Inverse Model	54
Figure 4.1: Bond Graph Model of Ball-on-Sphere System Without Causality	62
Figure 4.2: Causal Bond Graph of Ball-on-Sphere System	63
Figure 4.3: Validation of Ball-on-Sphere System using 20-Sim	66
Figure 4.4: Controllability Analysis of the Bond-on-Sphere System Bond Graph Model with Preferential Integral Causality	67
Figure 4.5: Controllability Analysis of the Bond-on-Sphere System Bond Graph Model with Preferential Derivative Causality	68
Figure 4.6: Observability Analysis of the Bond-on-Sphere System Bond Graph Model with Preferential Integral Causality	69
Figure 4.7: Observability Analysis of the Bond-on-Sphere System with Preferential Derivative Causality	70
Figure 4.8: Inverse Bicausal Bond Graph Model of the Ball-on-Sphere System	71
Figure 4.9: Model of Bond-on-Sphere System Decoupling Analysis	72
Figure 4.10: Result of Ball-on-Sphere Model Analysis	75

LIST OF TABLES

Table 3.1: The Parameters Description of the system model	41
Table 3.2: The physical Parameters of the System	58
Table 4.1: Comparison of ball-on-sphere system model with and without friction	75

LIST OF ABBREVIATIONS

Acronyms	Definition
BoS	Ball-on-Sphere
MIMO	Multiple Input and Multiple Output
SISO	Single Input and Single Output
MATLAB	Matrix Laboratory
FDI	Fault Detection and Isolation
20-Sim	Twente Simulation
SCAP	Sequential Causality Assignment Procedure
SCAPI	Sequential Causality Assignment Procedure for Inversion

CHAPTER ONE

INTRODUCTION

1.1 BACKGROUND

The ball-on-sphere system consists of the following basic components; a sphere, two motors, and two friction wheels (Moezi *et al.*, 2014) . The control objective of the system is to balance the ball on top of the sphere by controlling the rolling of the sphere along each of the two horizontal axes through friction wheels driven by motors. The control of the system is a challenging task because of its non-linear, unstable and under actuated nature (Ho *et al.*, 2009).

The ball-on-sphere is an important class of balancing systems with applications from robotics to transportation and aero-space in the following areas (Graf & Röfer, 2010):

- 1) missile guidance
- 2) modelling of a postural standing of human or humanoid robot
- 3) self-transport machine
- 4) modelling and simulation of the unstable system of a human or robotic upper limb
- 5) modeling and stabilization of space-ships and rockets

The ball-on-sphere system is as shown in Figure 1.1

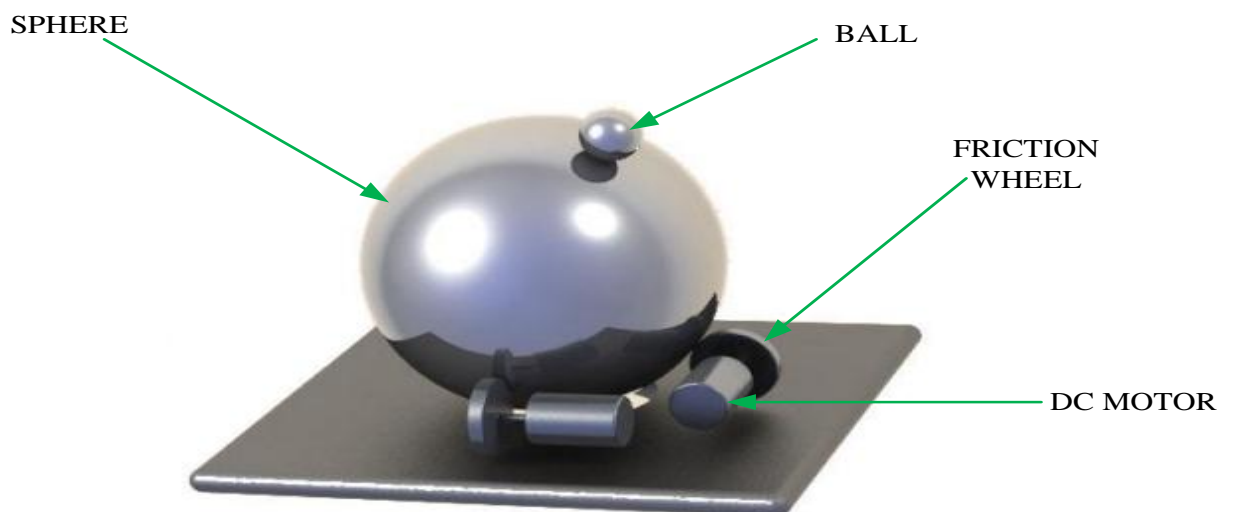


Figure 1.1: Ball on a Sphere System (Moezi *et al.*, 2014)

The dynamics of the ball-on-sphere system are nonlinear and complex and its parameters are interdependent in various directions; they have been considered to be two independent ball and wheel systems around the equilibrium point (Ho *et al.*, 2009). Parameter identification is among the most difficult steps in model design phase, which is the most cause of model errors (Dauphin-Tanguy *et al.*, 1999). The dynamics of ball-on-sphere system have been modeled using Euler-Lagrange modeling techniques. However, the existing method is limited with respect to not having detailed knowledge of the system's parameters (Moezi *et al.*, 2014). The dynamic equations of the ball-on-sphere system are non-linear and coupled, hence, it is normally difficult to obtain significant dynamics of the system using the various conventional numerical analytical tools.

Bond graph modeling technique captures most physical variables and dynamics of multi-domain systems. The bond graph model of the multi-domain systems help to overcome the mathematical complexities of conventional modelling techniques which are prone to errors (Borutzky, 2011).

The advantages credited to bond graph technique were explored in modelling the ball-on-sphere system in this work and in addition, were also used for the structural analyses of the system.

Several computer-based simulation tools are available for designing and simulating bond graphs. 20-Sim is a graphical modeling and simulation program which is suitable for generating and processing of dynamic systems (Alabakhshizadeh *et al.*, 2011). The 20-Sim is used to simulate and analyze bond graph models.

1.2 MOTIVATION

The modelling of multi-domains systems for control analysis and diagnosis is a major step in the design and simulation of multi-domains system (Paynter, 1970). Multi-

domain systems problem are interdisciplinary engineering systems problems, involving engineering systems in the domain of electrical, mechanical, chemical and amongst others. Modelling techniques such as variational and network graphic techniques do not have well defined uniform notations suitable for modelling and analyzing all type of physical domains systems (Yu & van Paassen, 2004). Bond graph technique provides uniform notation for physical systems and is based on energy and information flow in systems (Borutzky *et al.*, 2006). Furthermore, the technique has the capacity to carry out structural analysis in order to deduce information on a variety of structural properties of the system being model (Sueur & Dauphin-Tanguy, 1991). The Euler-Lagrange technique used in modelling the ball-on-sphere system is tedious and prone to modelling errors due to its computational complexities and does not have the capacity to analyze dynamic behavior of the system. Hence, the ball-on-sphere system requires a modelling technique that captures the various physical components of the system and provides a simple and efficient means for structural analysis and generation of dynamic equations of the system. These motivated the use of bond graph technique in this work. The bond graph technique is used to model and structurally analyze the ball-on-sphere system in order to study the dynamics of the system. This is because the method is based on the energy characteristics of each constituent physical component that contribute to the entire system developed (Karnopp *et al.*, 2012).

1.3 STATEMENT OF PROBLEM

Several attempts have been made to model the dynamics of the ball-on-sphere system. Researchers have used modelling technique such as Euler-Lagrange approach to model the system. However, the technique is prone to modeling error due to its computational complexities. The challenge had been that the dynamics of the system is nonlinear and complex and its parameters are interdependent on one another and are multi-directional

(Ho *et al.*, 2009). The existing model of ball-on-sphere system is limited for not having detailed knowledge of the system's parameters (Moezi *et al.*, 2014). Furthermore, the Euler-Lagrange technique does not have the capacity to carry out structural analysis of the information properties such as structural controllability and observability, inverse model and input-output decoupling of the ball-on-sphere model. Bond graph technique which is a suitable unifying concept that captures most physical variables and dynamics of the system was used to model the ball-on-sphere system. The bond graph technique was also used to carry out structural analysis of the ball-on-sphere system model properties in order to evaluate its dynamic behaviour.

1.4 AIM AND OBJECTIVES

The aim of this research is the modelling and structural analysis of the ball-on-sphere system using bond graph technique in order to study the dynamic behaviour of the system.

The objectives of the research are therefore as follows:

- 1) Development of bond graph model of the ball-on-sphere system.
- 2) Validation of the developed model in 1) using 20-Sim.
- 3) Implementation of the structural analysis of ball-on-sphere system using the bond graph technique in order to determine the structural controllability and observability, model inversion and input-output decoupling of the system.

1.5 DISSERTATION ORGANIZATION

The general introduction has been presented in Chapter One. The rest of the chapters are structured as follows: In Chapter Two, the literature review which comprises the review of similar works and the review of fundamental concepts pertinent to the research were presented. The fundamental concepts include ball-on-sphere system and its mathematical modelling, bond graph technique and structural analysis amongst

others. Chapter Three explains the bond graph technique method and procedures used in modelling and carrying out structural analysis of the ball-on-sphere system. The developed ball-on-sphere system bond graph model, the derived mathematical models describing the developed model and results of the structural analysis of the developed model were presented in Chapter Four. Finally, conclusion and recommendations of further work makes up the Chapter Five. The list of cited references and MATLAB codes in the appendix are provided at the end of this dissertation.

CHAPTER TWO

LITERATURE REVIEW

2.1 INTRODUCTION

In this chapter, the literature review which comprises the review of fundamental concepts of the ball-on-sphere system and the review of relevant similar works related to the system are presented.

2.2 REVIEW OF FUNDAMENTAL CONCEPTS

This section presents the review of fundamental concepts pertinent to the research, including ball-on-sphere system and its mathematical modelling, bond graph technique and structural analysis amongst others.

2.2.1 Ball-on-Sphere System

Ball-on-sphere is a class of multi-input multi-output (MIMO) nonlinear systems which is designed to control and operate a ball on the top of a sphere. Because of the inherent nonlinearity, instability and under actuation of this system, it often serves as a test bed for research in nonlinear control systems (Alireza *et al.*, 2014).

The system consists of a big sphere and a small ball. Over the surface of the sphere, a ball is to be stabilized by controlling the rotation of the sphere through two motors. According to the linearized model with respect to the equilibrium point, the system can be decoupled into two independent ball and wheel systems (Ho *et al.*, 2009), and this is said to be full state feedback linearizable (Liu *et al.*, 2011). The system finds application in modelling and stabilization of nonlinear control systems such as space-ships, humanoid robot and intercontinental missile guidance system.

2.2.2 Mathematical Model of Ball-on-Sphere System

Nonlinear control systems are those control systems where nonlinearity plays a significant role, either in the controlled process (plant) or in the controller itself (Binder

et al., 2009). Most physical systems are inherently non-linear (i.e. they do not satisfy two principles: superposition and homogeneity). A common engineering practice in analyzing a non-linear system is to linearize it about a nominal operating point and analyze the resulting linear model (Hassan, 2003). The ball-on-sphere model is non-linear and for ease of control and analysis it is expected to be linearized about an operating point. The operating point, at the instance of linearization, is that point at which all state and input variables are initialized to zero (Hassan, 2003).

Liu *et al.* (2011) developed a mathematical model of the ball-on-sphere system using the Euler Lagrange formulation by considering the following assumptions:

- 1) The ball rolls on the sphere without slipping.
- 2) The ball is always in contact with the sphere and
- 3) All frictional forces and torques are neglected

The basic feature of the ball-on-sphere system is shown in Figure 2.1

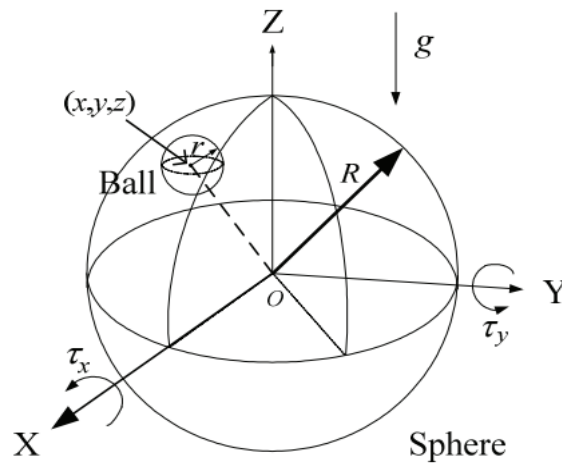


Figure 2.1: Ball-on-Sphere System (Liu *et al.*, 2011).

The parameters of the system as shown in Figure 2.1 are described as follows:

R is the Radius of the sphere; r is the radius of the ball; τ_x is the torque exerted in the x -axis direction; τ_y is the torque exerted in the y -axis direction; g is the gravitational force and (x, y, z) is the position of the ball.

The general form of Euler-Lagrangian equations used to describe the dynamics of the ball-on-sphere system is (Ho *et al.*, 2009):

$$\frac{d}{dt} \left[\frac{\partial L}{\partial \dot{q}} \right] - \frac{\partial L}{\partial q} = Q \quad (2.1)$$

where:

$L = T - V$ (Lagrangian function)

T: Kinetic Energy

V: Potential Energy

Q: Generalized forces

q: Generalized coordinates

For this system, q is selected as $q = [x \ y \ \alpha \ \beta]^T$, and Q is given by $Q = [0 \ 0 \ \tau_x \ \tau_y]^T$ (Ho *et al.*, 2009).

The dynamic equations are nonlinear and coupled, hence, it is difficult to find the dynamics of the system. However, from the linearized model with respect to the equilibrium point, the system can be decoupled into two independent subsystems as follows (Liu *et al.*, 2011)

$$\left[(R+r)m + I_b \frac{(R+r)}{r^2} \right] \ddot{x} - \left[I_b \frac{(R+r)}{r^2} \right] \ddot{\beta} - mgx = 0 \quad (2.2)$$

$$\left[-I_b \frac{R}{r^2} \right] \ddot{x} + \left(I_B + I_b \frac{R^2}{r^2} \right) \ddot{\beta} = \tau_y \quad (2.3)$$

$$\left[(R+r)m + I_b \frac{(R+r)}{r^2} \right] \ddot{y} - \left[I_b \frac{(R+r)}{r^2} \right] \ddot{\alpha} - mgy = 0 \quad (2.4)$$

$$\left[-I_b \frac{R}{r^2} \right] \ddot{y} + \left(I_B + I_b \frac{R^2}{r^2} \right) \ddot{\alpha} = \tau_x \quad (2.5)$$

Equations (2.2) and (2.3) represent the dynamics of the system in x-axis while equations (2.4) and (2.5) represent the dynamics of the system in y-axis.

Thus, near the equilibrium point the ball-on-sphere system can be decoupled into two independent ball and wheel systems. These subsystems are treated independently from each other and are controlled individually by a controller in the x and y axes, respectively. However, the dynamics equations for the ball and wheel system in the x and y-axes are identical (Liu *et al.*, 2011).

Consider the single-axis (ball-on-sphere) system as shown in Figure 2.2.

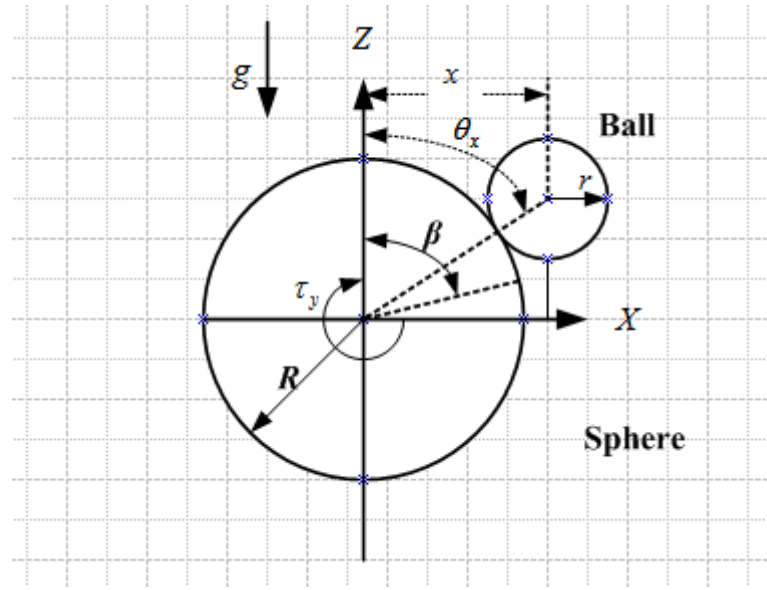


Figure 2.2: Ball-on-Sphere System in the x- Direction (Liu *et al.*, 2011)

The decoupled dynamics of the system into two independent ball and wheel systems are given by (Liu *et al.*, 2011):

$$\left[(R+r)m + I_b \frac{(R+r)}{r^2} \right] \ddot{\theta}_x - \left[I_b \frac{R}{r^2} \right] \ddot{\beta} - mg \sin \theta_x = 0 \quad (2.6)$$

$$\left[-I_b \frac{R(R+r)}{r^2} \right] \ddot{\theta}_x + \left(I_B + I_b \frac{R^2}{r^2} \right) \ddot{\beta} = \tau_y \quad (2.7)$$

2.2.3 Bond Graph Modelling Technique

Bond graph is a multi-domains modelling technique that simultaneously conveys the topological structure and the computational structure of the system being modelled.

Modelling and simulation of multi-domain systems, including interactions of physical effects from various energy domains, demand new approach (Paynter, 1970). Today's engineering domain is faced with increasing complex systems with evolving challenges whose solution depends on approaches that incorporate and considers all contributing subsystems to the task and cost function. As such, designers need system models that can be constructed using a uniform notation technique for all types of physical systems.

Bond graph method is based on energy and information flow in systems. Some applications and fundamentals of bond graph are found in (Borutzky *et al.*, 2006) and (Karnopp *et al.*, 2012). In Kayani and Malik (2008), it was established that bond graph technique is a tool that can be used to model systems with different energy domain characteristics. Similarly, for concurrent modelling of mechatronic systems, Borutzky *et al.* (2006) demonstrated the usefulness of bond graph as a multi-domain modelling technique. The bond graph as a modelling tool is a simple and elegant approach that takes into account multi-energy exchange in systems. The technique is less prone to errors, as such, will be applied in this work for modeling the ball-on-sphere system.

A bond graph consists of subsystems connected together by lines representing power bonds. Each process is described by a pair of variables, effort (e) and flow (f), and their product is the power. The direction of power is depicted by a half arrow. The technique takes into account power and energy exchange on multi-domain combination of systems such as mechanical, electrical, hydraulic, and biological, etc. Bond graph methodology is a graphical notation of energy port-based description for modelling dynamic systems (Kayani & Malik, 2008). Each bond has a vertex and an edge; the vertices represent sub-models A and B while the edge stands for the energy connection between power ports.(Borutzky *et al.*, 2006). This is as shown in Figure 2.3.

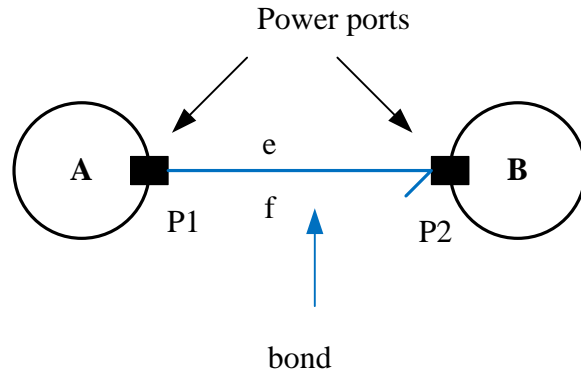


Figure 2.3: Schematic Diagram of Energy (Borutzky *et al.*, 2006)

Bond graph is a unique technique for multi-domain systems modelling as it provides a systematic method for representing the interconnection of multi-energetic system elements. It provides room for expansion, incorporation of new sub-models in an existing one, efficient structural analysis, fault detection and isolation (FDI) capabilities. Bond graph is easily incorporated and compatible with most simulation software's, like 20-sim, Simulink/Matlab, Dymola and labVIEW (Ngwompo, 2011).

The advantages of bond graph modelling over other modelling techniques such as variational and network techniques are as follows (Yu & van Paassen, 2004):

- 1) It is a unique language for all physical domains.
- 2) Its models are easier to understand in terms of the physical relation between components.
- 3) It clearly shows the cause and effect relations in the model.
- 4) It allows further possible development and evolution of the model.
- 5) It is also a tool for analyzing the system's structural properties.
- 6) It conveys the transfer of energy, power and information between subsystems.
- 7) It has computer aided modelling support.

Some of the drawbacks of bond graph method are as follows (Yu & van Paassen, 2004):

- 1) Bond graphs key properties are not well defined with exact meaning of specific symbols.
- 2) It has no toolbox available for mathematical analysis.

2.2.3.1 Bond graph modeling implementation

The bond graph procedures of modelling systems include the following steps: (Benmoussa *et al.*, 2014)

- 1) Identification of the various subsystems, storage elements (e.g. moment of inertia parameters), the dissipating elements (e.g. frictional parameter) modelled as loss of free energy and sources of energy (e.g. torque) of the system being modelled.
- 2) Identification of the various junction structures which are the energy distribution in the system i.e. the 1-junctions and 0-junctions.
- 3) Insertion of 1-junctions to the identified distinct angular velocities of the system.
- 4) Identification of the reversible transformation of energy (TF) element i.e. separately relating the efforts at the ports and the flows at the ports of the system.
- 5) Attachment of a reference direction for the energy flow to each bond (half arrow).
- 6) Mapping out and connecting the causal bonds of the system components with appropriate causality assignment.
- 7) Simplification of the bond graph structure by removing all 1-junctions representing an angular velocity identical to 0-junction along with all incident bonds.

2.2.4 Causality Concept

In bond graph theory, the concept of causality is important. This refers to cause (input) and effect (output) relationship. Thus, in the process of bond graph modelling, causality assignment plays an important role, which is implicitly introduced and it is graphically represented by a short stroke, called causal stroke, placed perpendicular to the bond at

one of its ends indicating the direction of the effort variable. Causal stroke assignment is independent of the power flow direction. The concept leads to generation of state space equations from the bond graph structure.

The decision to make which of the component models to reflect the causality is systematic and energy directed. Figures 2.4 to 2.6 show the possibilities of causality assignment for the given elements. For storage elements such as Inertance (I) and Capacitance (C), integral causality is preferred.

The design of causality for a capacitance component is as shown in Figure 2.4a and Figure 2.4b. Figure 2.4a structure shows integral causality configuration while Figure 2.4b shows differential causality configuration.

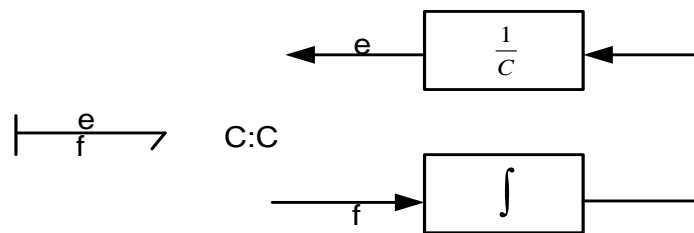


Figure 2.4a: Capacitance (C) Causality Integral Configuration (Borutzky *et al.*, 2006)

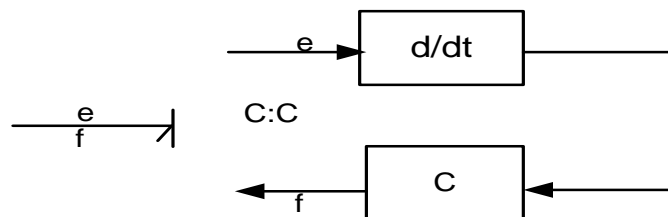


Figure 2.4b: Capacitance (C) Differential Configuration (Borutzky *et al.*, 2006)

For the design of causality of an inertance component, Figure 2.5a and Figure 2.5b show the two variants. Figure 2.5a shows integral causality configuration while Figure 2.5b shows the differential causality configuration.

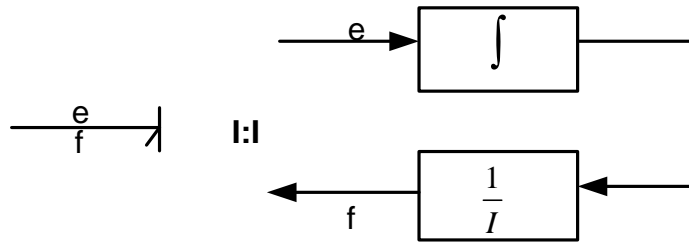


Figure 2.5a: Inertance (I) Causality Integral Configuration (Borutzky *et al.*, 2006).

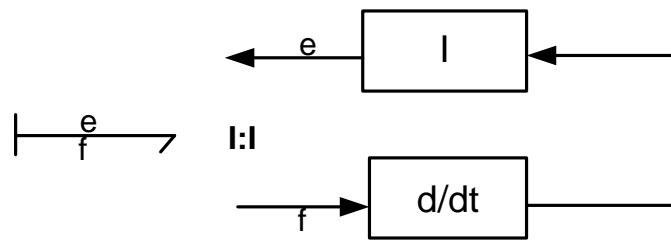


Figure 2.5b: Inertance (I) Causality Differential Configuration (Borutzky *et al.*, 2006).

For the design of causality of resistance component of a system, Figure 2.6a and Figure 2.6b show the two variants. Figure 2.6a shows integral causality while Figure 2.6b shows differential causality configuration of the resistance variant.

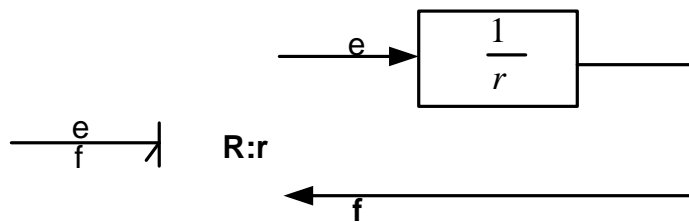


Figure 2.6a: Resistance (R) Causality Integral Configuration (Borutzky *et al.*, 2006).

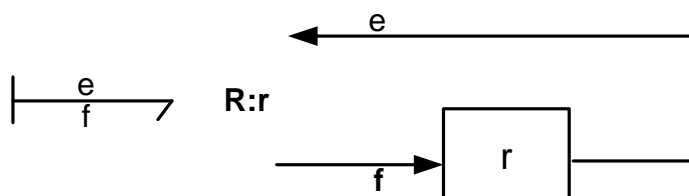


Figure 2.6b: Resistance (R) Differential Configuration (Borutzky *et al.*, 2006).

In bond graph theory, models of various systems belonging to different engineering domains can be expressed using a set of only nine elements, called elementary components (Bobaşu *et al.*, 2010). A classification of bond graph elements can be made up by the number of ports. The ports are places where interactions with other processes take place.

The one port elements are represented by the following bond graph elements:

Effort sources (Se) and flow sources (Sf), e.g. Electric mains (voltage source), gravity (force source), pump (flow source)

- 1) Inertance (I), Storage element for a p-type variable, e.g. inductor (stores flux linkage), mass (stores momentum).
- 2) Capacitance (C), Storage element for a q-type variable, e.g. capacitor (stores charge), spring (stores displacement).
- 3) Resistance (R) dissipating free energy, e.g. Electric resistor, mechanical friction.

While the two ports elements are represented as

- 1) Transformer (TF), e.g. an electric transformer, toothed wheels, and lever.
- 2) Gyration (GY), e.g. electro-motor, centrifugal pump.

And the multi-ports elements are effort junctions and flow junctions represented as

0 – junction and 1 – junctions, for ideal connection of two or more sub-models.

2.2.4.1 Sequential causality assignment procedures

The sequential causality assignment procedure (SCAP) provides rules to be followed in assigning computational causalities at power ports of bond graph model as follows:

- 1) Causality assignment to the sources of energy. The causal information is to be propagated into the bond graph through its junction structure as far as possible by observing causality rules at element ports.

- 2) Step 1 will be repeated until all ports of sources are assigned an appropriate causality.
- 3) Preferential integral causality is next to be assigned to the ports of the storage elements e.g. the moment of inertia. The causal information will be propagated into the bond graph.
- 4) The causality assignment procedure continued with assigning causality to the dissipating element e.g. the frictional force with characteristics that do not have a unique inverse.
- 5) Finally, causality will be arbitrarily assigned and propagated through the junction structure. This fifth step will be repeated until no causally unassigned bonds are left on the bond graph model. (Borutzky *et al.*, 2006).

2.2.4.2 Derivation of equations from systems causal bond graphs

A mathematical model describes the dynamics of the system being modelled with respect to the integrals of the storage elements which are the state variables of the system. The following steps describe the order of deriving sets of differential equations from systems causal bond graph structures:

- 1) The constitutive equations for all the independent sources of energy are to be written with their outputs given in functions of time.
- 2) The input by contrast is algebraically related to its controlled source output. If the former is not an output of an independent source or an energy store with integral causality, then it can be represented by means of such outputs by back propagation of causal paths in the junction structure and by eliminating intermediate variables.
- 3) The resistors outputs depend algebraically on their inputs. By propagating backward along causal paths through the junction structure, their outputs can be expressed by sources either independent or controlled ones or outputs of energy stores. The

outputs of dependent sources do not need to be eliminated, since they have already been determined in the previous step

- 4) The derivative with respect to time of an output is a function of the input(s) for the storage elements ports. By working back causal paths, the inputs can be expressed by outputs of other energy stores, of resistors, or sources. (Borutzky *et al.*, 2006)

2.2.5 20-Sim Software

20-sim is an application developed for the analysis and simulation of dynamics systems. The purpose of 20-sim is to support the engineer in the process of design, analysis and diagnosis of engineering systems using modelling and simulation (Broenink, 1999). It is a modelling and simulation program that is compatible with Microsoft Windows, Linux and Mac Operating software. With this program, the behaviour of multi-domain dynamic systems such as electrical, mechanical and any mechatronic systems can be simulated and analyzed.

The 20-sim program has the capacity to interact across other modelling and simulation based software such as MATLAB, Modelica, labVIEW, Dymola, and others. Its tool boxes includes; Bond graph Toolbox, Mechanics Toolbox, Animation Toolbox, Time Domain Toolbox, Frequency Domain Toolbox, Control Toolbox, Mechatronics Toolbox, Real Time Toolbox, (Broenink, 1999). Figure 2.7 shows the graphical user interface of the 20-Sim software.

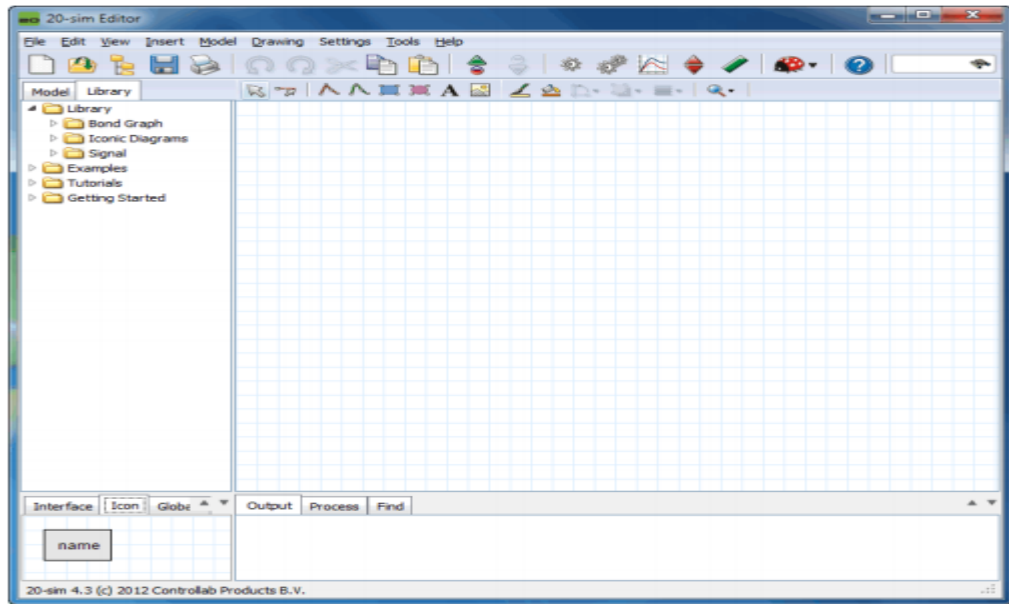


Figure 2.7: 20-Sim Graphical User Interface (Mahindrakar & Kulkarni, 2012)

The 20-Sim graphical interface is an interactive tool, where model entry and model processing and model validation are fully integrated (Broenink, 1999). As such, it gives feedback as early as possible in the modelling process, which enhances the quality of the tool. Dynamic systems can be built and validated by choosing components from bond graph library and connecting them together. The Model tab shows the model hierarchy, i.e. the composition of all the elements of the model. The Library tab shows the bond graph 20-sim library (Mahindrakar & Kulkarni, 2012). The 20-Sim package has advanced support for bond graph modelling making it well rated in the bond graph community. 20-sim can be categorized as a fully integrated modeling and simulation environments especially supporting bond graphs when compared with other modelling tools like Simulink and Labview (Borutzky, 2011). The advantage of 20-sim is the direct input of bond graphs in 20-sim and the availability of built-in tools for system dynamic analysis and 3D mechanical modelling. According to Ledin (2001), 20-sim differs from other simulation tools like Simulink and VisSim in that it supports four methods for modelling dynamic systems: iconic diagrams, block diagrams, bond graphs and equations.

2.2.6 Structural Analysis Concept

The structural analysis by bond graph approach of linear time-invariant systems was introduced by Dauphin-Tanguy *et al.* (1999), Karim *et al.* (2003) and Rahmani *et al.* (1996) to simplify decoupling study of systems and therefore, structural analysis defines the necessary conditions that are valid for most values of numerical parameters. Structural analysis is usually performed during the system design phase and is used to deduce information on a variety of structural properties, such as: system controllability, observability, diagnosability, stability, invertibility etc. for the control designer.

Sharon *et al.* (1991) proposed that control system design could, and should, be based on physical system insight. Bond graphs provide a high-level modelling language for describing dynamic systems in a graphical form which retains such physical insight. Sueur and Dauphin-Tanguy (1989) established the structural analysis of bond graphs using concepts from control theory. Since many well-known results from control theory typically use the linear time invariant state space representation for numerical analysis, it follows that this representation can be obtained from the structural properties of bond graph structure (Sueur & Dauphin-Tanguy, 1991).

The subsections as follows review the basic information from structural properties analysis of bond graph structure.

2.2.6.1 Controllability concept

Controllability of systems is a basic concept for analyzing and designing systems using modern control theory (Burns, 2001). Controllability is simply checking if every state variable $x(t)$ is or not can be controlled by input variable $u(t)$, by analyzing the control ability of $u(t)$ to state variables $x(t)$. The conventional approach to determining controllability for linear system is by showing that the Kalman controllability matrix which is defined as $M_c = [A:AB:\dots:A^{n-1}B]$ is of full rank i.e.it has n-linearly

independent columns (Burns, 2001). This approach requires using the state-space model and it heavily depends on parameters of A and B matrices. Furthermore, it requires higher computations if the numbers of state variables are large. Comparing with conventional numerical matrix method, bond graph method does not depend on parameters of state matrices A and B and it overcomes miscellaneous computation for obtaining controllability matrix. Bond graph contains system structure properties and can determine state variables.

In bond graphs concept, structural controllability has been used as a more physically meaningful parameter than classical state controllability. Dauphin-Tanguy *et al.* (1999) and Sueur and Dauphin-Tanguy (1991) used the bond-graph technique to derive information on structural controllability properties for the design of control systems.

According to Sueur and Dauphin-Tanguy (1991), for a bond graph model to be structurally controllable, two conditions have to be satisfied:

- 1) There exists at least a causal path linking each dynamical element in integral causality and a control source in the bond graph in preferential integral causality,
- 2) All the dynamical elements in integral causality in the bond graph in preferential integral causality accept a derivative causality when a preferential derivative causality is assigned on the bond graph model. If it is not satisfied directly, a dualization of some input sources has to be performed in order to transform the remaining integral causalities.

2.2.6.2 Observability concept

A system is completely state observable, if the Kalman observability matrix

$M_o = [C^T : A^T C^T : \dots : (A^T)^{n-1} C^T]$ is of full rank i.e. it has n-linearly independent rows

(Burns, 2001). Several works have been presented using bond graph methodology to

derive information on structural observability properties for control systems design, these include Galindo *et al.* (2006) and Sueur and Dauphin-Tanguy (1989).

In the structural observability analysis, detector elements are typically added to the bond graph to give an output field and these elements are used to observe the system. Observability is the dual property of controllability.

Sueur and Dauphin-Tanguy (1991) established that for a bond graph model to be structurally observable, two conditions have to be satisfied:

- 1) There exists at least a causal path between each dynamical element in integral causality and a sensor in the bond graph in preferential integral causality,
- 2) All the dynamical elements in integral causality in the bond graph in preferential integral causality accept a derivative causality when a preferential derivative causality is assigned on the bond graph model. If it is not satisfied directly, a dualization of some input sources has to be performed in order to transform the remaining integral causalities.

2.2.6.3 *Bi-causality concept*

Conventional bond graph theory is predicated on the notion that a bond has a single causal stroke i.e. an effort imposed at one end implies a flow imposed at the other end (Gawthrop, 1994). This notion is implied by components having a known constitutive relationship.

Bi-causal bond graphs were introduced by Gawthrop (1994) as an extension of conventional bond graph theory, in order to handle systems with non-standard input-output patterns. This gives foundation for deriving system properties relating to system inversion, state estimation and, parameter estimation, directly from the system bond graph. The concept of causality relies on the idea that physical components cannot impose both conjugate power (flow/effort) variables to its connected subsystem. A bi-

causal assignment extends the concept of causality by allowing both conjugate power (flow/effort) variables to its connected subsystem. To represent the bi-causality, the causal stroke is divided in two, as depicted in Figure 2.8. From the figure, it is shown that effort and flow information paths are co-oriented (dashed arrows).

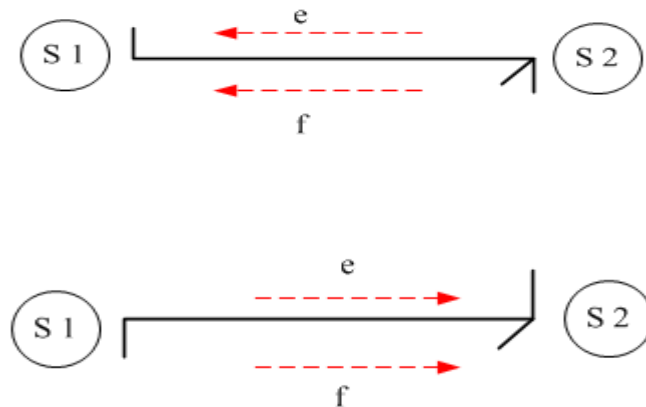


Figure 2.8: Bi-causal Bond Graph for Physical Subsystems (S1, S2) (Gawthrop, 1994)

2.2.6.4 Model inversion concept

Contrarily to direct model, an inverse model is used to know which inputs are required given the desired outputs. The inverse of a dynamic system is defined as the new system which, given the initial system output as its input, will exactly reproduce the system input as its output for the purposes of design and synthesis of control systems (Gawthrop, 1994). Control design based on such inverse system models are used in a number of application domains. In robotics, the inverse models of computed-torque and feed forward manipulator control techniques (An *et al.*, 1988; Craig, 2005) are used to give the joint torques required to give a pre-specified manipulator trajectory. In process engineering, internal model control (Morari & Zafiriou, 1989) generic model control (Lee & Sullivan, 1988) exact linearization strategies (Henson & Seborg, 1991) all implicitly use the notion of inverse models and the corresponding ideal control. In flight control, nonlinear inverse dynamics have been used as a basis for control design (Lane

& Stengel, 1986). The inverse of a system has independent interest for revealing properties of the system itself (Kailath, 1980).

Bond graph as a modeling tool has proven to be a powerful tool not only for modelling the direct model of a system but also to obtain its inverse model. The inversion of bond graph model uses the bi-causal concept (Gawthrop, 1998). The idea of using the bi-causality for system inversion is motivated by its computation capabilities. Figures 2.9 and 2.10 show a general representation of the bond model for direct and inverse system respectively.

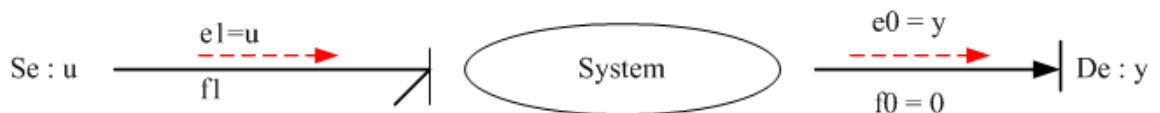


Figure 2.9: General Representation of a Bond Graph Direct Model (Gawthrop, 1994)

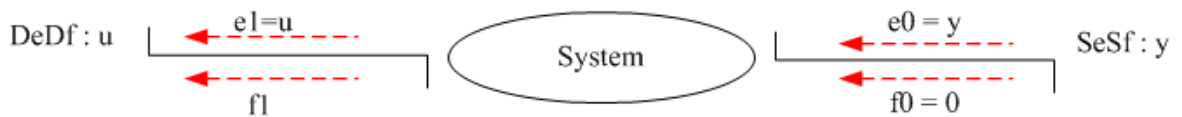


Figure 2.10: General Representation of a Bond Graph Inverse Model (Gawthrop, 1994)

Procedures for bicausality assignment for model inversion (SCAPI):

- 1) In bond graph model with preferential integral causality, a set of disjoint input/output power lines associated with a set of disjoint input/output causal paths are selected.
- 2) In an acausal bond graph model, the source elements (and detectors) associated to the inputs (and outputs) are replaced by double detector DeDf (and double source SeSf).
- 3) For each element of which causality is imposed (i.e. sources, elements with noninvertible constitutive laws), they are assigned with their causalities and the causalities are propagated through the junction structure, taking into account the causality constraints of 0-junctions and 1-junctions and transformer (T F) elements.

- 4) On the first step, along each power selected, the bi-causality are propagated from the double source to the double detector and the causality via the junction structures are also propagated while taking into account the causality constraints of 0-junctions, 1-junctions and transformer (T F) elements.
- 5) Choose any energy storage element without causality, and assign a preferential integral causality to it. Propagate the causality as far as possible until all storage elements are causal.
- 6) If some R-elements remain not causally determined, assign causality to one and propagate it as previously. Repeat this step until all R-elements are causally determined.
- 7) If the bond graph model is not completely causally determined, assign causality on a bond and propagate it as previously. Repeat this step until all bonds are causally determined. (Ngwompo *et al.*, 1997)

2.2.6.5 Input-output decoupling concept

Porter (1969) presented conventional procedure for input-output decoupling of linear time-varying systems. The algorithm is defined for numerical purposes which are separated into two parts; the analysis and the synthesis of the decoupling law.

The input-output decoupling problem has received much attention since the first development proposed in (Falb & Wolovich, 1967). This problem is usually decomposed in several steps such as: input-output decoupling study, control law calculus (decoupling matrices) and analysis of the stability property of the controlled model.

The first development was concerned with linear models from a state representation. Porter (1969) proposed an extension to the time-varying models and later similar approaches to nonlinear models have been proposed.

A bond graph approach was first proposed for linear models in Bertrand (1997). The input-output decoupling problem was solved with the concept of causal paths and the control law expression was characterized with the joint application of the geometric approach and the graphical approach. The stability of the controlled model was then studied.

2.3 REVIEW OF SIMILAR WORKS

This subsection presents a review of works carried out by researchers to model and analyze the ball-on-sphere system and related systems.

Galindo *et al.* (2006) considered structural controllability and observability analysis of closed loop linear time invariant multi-input multi-output stable systems modeled in bond graph which are described by their junction structures. The juncture structures were function of the free parameter of the family of stabilizing compensators and it allowed achieving necessary and sufficient conditions for structural controllability and observability of the bond graph model in closed loop. The free parameter was gotten from its state space realization, for single-input single output systems. However, analyses such as input-output decoupling were not considered in the model structural analysis study in order to determine whether the system can be decoupled or not.

Matsuda and Ohse (2006) employed the ball and wheel system model and derived the mathematical equation for the dynamic analysis of the system and its implementation for designing a dynamic controller for the control of the system. The researchers approached the synthesis problem by first deriving the mathematical model of nonlinear plant with sector-bounded nonlinearity. Secondly, the analyses conditions for systems with sector-bounded nonlinearity were introduced, and based on these conditions the synthesis problem was formulated as a bilinear matrix inequality. However, there were

difficulties in synthesizing a controller for nonlinear systems with sector-bounded nonlinearities.

Ho *et al.* (2009) presented the derivation of the mathematical model of the ball and wheel system by using the Euler-Lagrange formulation. In the work, considerable assumptions were made during the modelling process in order to represent the basic features of the dynamics of the system. Feedback linearization was used to transform the nonlinear system into a linear time-invariant system in controllable canonical form for the purpose of numerical analysis of the system dynamic behaviour. However, feedback linearization employed for the analysis of the model was limited due to the requirement of the exact model of the dynamics of the system.

Bobaşu *et al.* (2010) carried out bond graph detailed modelling and the design of feedback linearizing technique applied to an inverted pendulum system. In the modelling of the system using bond graph technique, the following steps were adopted: the first step was to write a word bond graph which contains words instead of standard symbols for the main components, and bonds for power and signal exchange of the system. The next step was to replace words by standards elements which contain precise mathematical or functional relations. The system was decomposed into three subsystems that were modeled separately: dc motor, gear and inverted pendulum. 20sim modelling environment was used to create and validated the developed model. The mathematical equations derived were used to formulate the state space equations starting from the constitutive relations of elements for the system analysis. However, in the work, bond graph based structural analyses of the developed model were not considered in order to study the underlying dynamic behaviour of the system.

Orlikowski and Hein (2011) used a uniform, port-based approach in modelling beam/bar systems using bond graph technique. The port-based model of such a

distributed parameter system was by application of the bond graph methodology. The considered beam/bar systems were assumed to be composed of one dimensional distributed parameter systems. For each element, there exist four possible displacements: longitudinal, transverse displacements in two perpendicular planes and torsional displacement. Considering the elements making up the overall structure, the overall mathematical model was formulated by application of partial differential equations with appropriate boundary conditions dependent on external fixing and connections between the elements. In the work, structural analyses of the system were not carried out using the bond graph technique in order to study the system dynamic behaviour.

Mohammad and Khashabi (2011) worked on the modelling of ball and plate system for stability analysis of the system. In the work, exact non-linear differential equations of the ball and plate system were first derived by the use of Lagrange-Euler equations. The nonlinear equations of the model were then transformed to linear model for the purpose of dynamic behaviour analysis of the system. The motor model was also presented in the work to show the effect of external torque on the ball-on-plate system. However, considering the assumptions made in the modelling process, not all forces acting on the system were considered.

Liu *et al.* (2011) presented a modelling approach for obtaining nonlinear model of the ball-on-sphere system using Euler-Lagrange modeling technique. The Euler-Lagrange technique was used to obtain the translational and rotational dynamics for the nonlinear system model. In the work, feedback linearization was used to transform the nonlinear model of the system to linear model for the system analysis. However, the developed model did not take into consideration the resolution of all the forces acting on the ball such as the frictional force.

Bambagini and Di Natale (2012) carried out a detailed mathematical modelling of ball and plate system. The modelling determined the dynamic equations on the basis of the Newton's laws of motion to compute the motion equations of the system. The model took into account both its structure and some forces acting on the system. The presented equations of the dynamics of the system were continuous, non-linear and coupled. However, not all the moments and forces acting on the system were considered in the modelling process.

Deur *et al.* (2012) presented an overview of the bond graph modelling of an advanced automotive transmission and driveline systems. This included one-mode and two-mode series-parallel hybrid electric vehicle transmissions, a continuous variable transmission, active-limited slip and torque vectoring differentials in two-wheel drive (2WD) and four-wheel drive (4WD) configurations, and electromechanical actuator-based wet and dry clutch actuation systems. In the work, bond graph method was effectively used to gain valuable insights about the system dynamics structure and behaviour. However, structural analysis of the developed model using bond graph was not considered in the study in order to understand the dynamic behaviour of the system.

Zakeri *et al.* (2012) worked on the model of ball-on-sphere system for the purpose of designing a nonlinear adaptive feedback linearization for stability analysis of the nonlinear system. Adaptive feedback linearization was used to update the system's parameters by a suitable update law for stability analysis for the system. However, one of the most difficult steps in the model design phase was the parameter identification, which was the main cause of modelling errors. As such, the technique was inadequate to give thorough analysis of the system parameters.

Willson *et al.* (2012) presented the model of ball and wheel system using analytical mechanics. The model considered the dynamics of a ball running on a grooved wheel

and the influence of the groove angle on the ball. The system nonlinear model developed was transformed to a linear model using feedback linearization for the purpose of analysis. Quotient method which was an algorithmic method was used to design control law for stability analysis of the system. However, the algorithmic procedure used for the system analysis was tedious and prone to error as the process required various iterations for obtaining the control law for the system.

Chikhaoui *et al.* (2013) used an energetic method of helicopters dynamics analysis to study the air resonance (AR) phenomena using bond graph technique. In the work, a brief state-of-art of AR phenomena was presented and part of the state-of-art was devoted to the bond graph modeling method showing several advantages of the tool. The work proposed a macroscopic energy description of the system through the word bond graph representation. The bond graph was used for rotor/fuselage structure modelling in order to study the AR phenomena instability. The 20-Sim software was used to validate the developed model. However, the graphical model of the system was not exploited in order to facilitate analysis of its structural properties.

Ho *et al.* (2013) modelled the dynamics of the ball-on-sphere system using Lagrange approach. The dynamics of the system presented were coupled and nonlinear. Hence, the system was simplified based on two decoupled ball-and-wheel system. To simplify the developed nonlinear model of the system, the predominant nonlinear terms of the ball and wheel system were retained, but the high order coupling terms were neglected. The simplified model was used for controller design for the purpose of stability analysis of each decoupled system. However, the developed model did not take into consideration the resolution of all the forces acting on the system such as the frictional force.

Rebecca and Margetts (2013) implemented modelling and structural analysis of hybrid dynamic systems using bond graph approach. In the work, a hybrid bond graph method was proposed for analysis as well as providing engineering insight through the choice of controlled elements and dynamic causality. Hybrid models are those describing both continuous and discontinuous behaviour of systems. They carried out detailed study of controllability and observability structural analysis of the hybrid dynamic systems. However, model inversion analysis of the hybrid dynamic systems was not considered in the study.

Moezi *et al.* (2014) used the model and the derived dynamical equations of the ball-on-sphere for the purpose of fuzzy logic control of the system. The dynamical equations presented were nonlinear and their parameters interdependent in various directions. To address the complexities, the system was considered to be two independent ball and wheel systems around its equilibrium point, since at that point, the parameters were assumed independent in all directions. However, the proposed technique was not adequate for stability analysis of the ball-on-sphere model due to the complex dynamics of the system. As such, parameters and their bound limit were defined by intuition which of course did not represent the real dynamics of the system.

Alireza *et al.* (2014) proposed the model and the dynamic equations of the ball-on-sphere system for the design and analysis of the system. In the work, an adaptive neural network technique was used for the purpose of the system stability analysis based on the developed model. The nonlinear nature of the physical dynamics of the system and its parameters, which were interdependent on one and others, made the modelling of the system difficult. However, the process of obtaining the system model for stability analysis of the system was prone to error due to the complexity of the system dynamics.

The modelling errors made the controlling technique used to design control law for the system analysis ineffective for the system analysis.

It is evident from the literatures reviewed that the Euler-Lagrange technique is prone to modelling error due to its computation complexities and limited in its capacity to carry out structural analysis of the information properties of the ball-on-sphere system. In this research work, bond graph technique was used to model and carry out structural analysis of the ball-on-sphere system in order to study the dynamic information properties of the system and to minimize the mathematical complexities of the modelling process.

CHAPTER THREE

METHODS AND MATERIALS

3.1 INTRODUCTION

In this chapter, the methods, materials and procedures used for the successful completion of this research are explained and these involve modelling and structural analysis of the ball-on-sphere system using bond graph technique.

3.2 METHODOLOGY

The following steps describe the methodology adopted in this research work:

- 1) Modelling of the ball-on-sphere system using bond graph technique.
 - a) Identifying the various subsystems, energy exchange, power transfer and storage elements of the ball-on-sphere system.
 - b) Identifying the junction structure of the system i.e. 0, 1, and transformers (TF) elements.
 - c) Mapping out the bonds and applying causality appropriately.
- 2) Validation of the model developed in 1) using 20-Sim
 - a) Identifying the model components from the bond graph library.
 - b) Building the ball-on-sphere model by connecting the identified components and verifying causality assignment.
 - c) Processing and diagnosis of the model to ensure that its error free.
- 3) Structural analysis of the ball-on-sphere system using bond graph technique.
 - a) Introducing bi-causality concept for inverse model of the system.
 - b) Using source-sensor elements, dynamical elements and detectors for controllability and observability analysis of the system.

3.3 BALL-ON-SPHERE MODELLING

This section explains the bond graph modelling, causalities assignment and equations derivation procedures of the ball-on-sphere system.

3.3.1 Bond Graph Modelling of Ball-on-Sphere System

The advantages presented by the bond graph modelling approach are employed in modelling the ball-on-sphere system.

The following steps explain the procedures involved in the development of the bond graph model of the ball-on-sphere system:

- 1) First of all, the ball-on-sphere system was decoupled into two subsystems ball and wheel systems in x axis as shown in Figure 3.1. This simplified the modelling and physical parameter identification of the system.

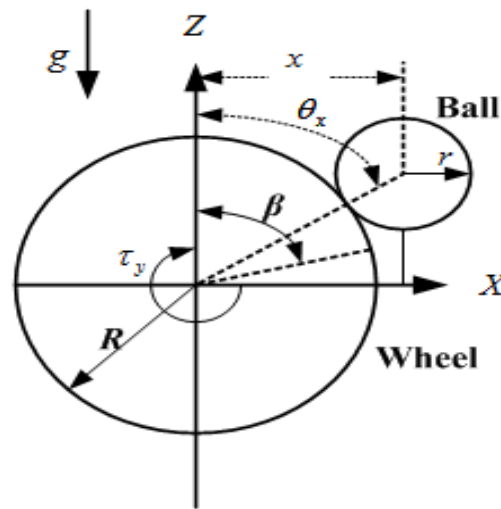


Figure 3.1: Ball and Wheel System in x-axis (Ho *et al.*, 2013)

- 2) The various physical components of the system were identified and modelled. These include the storage elements i.e. moment of inertias (J_s , J_b and I_b), the dissipating element i.e. frictional parameter (B) and transformers (T_1, T_2 and T_3) ports were inserted via a 0-junction between two 1-junctions.

- 3) The source of energy connected to system i.e. motor ($U1$) and the gravitational force ($U2$) acting on the ball were identified and attached to their appropriate 1-junctions.
- 4) Furthermore, the distinct angular velocities (ω_s and ω_b) of the sphere and ball were identified and represented by a 1-junction respectively.
- 5) The inertias elements were attached to their respective 1-junctions.
- 6) Power bonds were assigned as a reference direction to connect the identified physical components of the system in order to specify the flow of energy within the system.
- 7) Finally, the bond graph model of the ball-on-sphere system was simplified by removing all 1-junctions representing an angular velocity identical to 0-junction along with all incident bonds.

These set of procedures were used to develop the acausal bond graph model (i.e. bond graph model without causality) of the ball-on-sphere system. The developed acausal model shows the dynamics of the system as the ball rotates and revolves round the rotating sphere due to the applied torque.

3.3.2 Ball-on-Sphere System Causalities Assignment

This subsection explains the procedures involved in assigning causalities to the acausal bond graph model of the ball-on-sphere system. The sequential causality assignment procedure (SCAP) was followed in assigning causalities to the ball-on-sphere system acausal model.

These steps described the procedures involved in the appropriate causality assignment on the ball-on-sphere system:

- 1) Causalities were assigned to the sources of energy i.e. the motor and the gravitational force which act on the ball. The causal information was propagated

into the bond graph through its junction structures as far as possible by observing causality rules at element ports.

- 2) Step 1 was repeated until all ports of sources were assigned an appropriate causality.
- 3) Preferential integral causalities were assigned to the ports of the moment of inertia of sphere and ball which are the system's storage elements. The causal information was propagated into the bond graph.
- 4) The causality assignment procedure continued by assigning causality to the dissipating element i.e. the frictional parameter with characteristics that do not have a unique inverse.
- 5) Finally, causalities were arbitrarily assigned and propagated through the junction structure i.e. the 0-junctions and 1-junctions. This step was repeated until no causally unassigned bonds are left on the ball-on-sphere system model.

The ball-on-sphere system bond graph model with appropriately assigned causality specified the cause and effect relationship in the system. Furthermore, mathematical model of the ball-on-sphere system can be derived from the causal bond graph model.

3.3.3 Ball-on-Sphere System Equations Derivation

In this subsection, the procedures involved in obtaining the mathematical model of the ball-on-sphere system from the causal bond graph model are explained. The equations of the ball-on-sphere system were derived in three steps as follows:

- 1) The constitutive equations of what the independent sources, inertias and resistive elements contribute to the ball-on-sphere system were derived by observing the associated causalities and using variables for strong bonds.
- 2) The relative equations of the system's junction structures i.e. the 0-junctions and 1-junctions and the two-port elements i.e. transformation ratios (TF) were also derived for the variables with the strong causal bonds.

- 3) The system variables which were expressed in terms of states in other derived equations were replaced in the process of deriving the mathematical model. Continuous sorting and replacement was done until the entire sets of equations were expressed in terms of states and system parameters only.

These sets of procedures were followed in deriving the mathematical model of the ball-on-sphere system from the developed causal bond graph structure of Figure 3.2. Important consideration was made with respect to the directions of flow and effort in deriving the equations. These considerations include:

- 1) What each element in the causal bond graph is contributing to the system
- 2) What the system gives back to each storage element in preferential integral causality

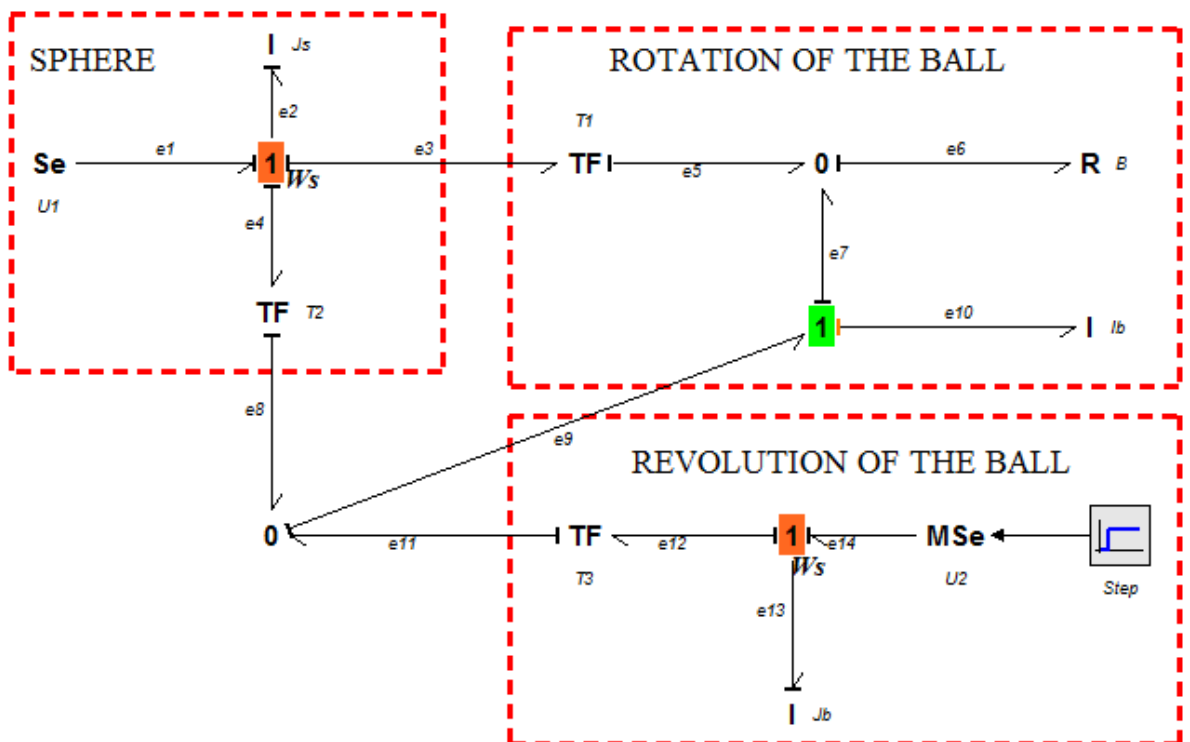


Figure 3.2: Bond Graph Structure of Ball-on-Sphere System

Step 1: Internal equations; the elements in preferential integral causality i.e. the source element which supply an input (τ_y), the independent storage elements (I_s and I_b) and

the resistive element (B) generate the following set of equations relating efforts (e) and flows (f):

$$I_s = J_s$$

Therefore, from Figure 3.2, the following equations are derived:

$$\left. \begin{aligned} \tau_y : e_1 &= s e_1 = \tau_y \\ I_s : f_2 &= \frac{p_2}{I_s} \\ B : e_6 &= B f_6 \\ I_b : e_{10} &= I_b \dot{f}_{10} \\ I' : f_{13} &= \frac{p_{13}}{I' = m(\mathbf{R} + \mathbf{r})^2} \\ e_{14} &= mg \sin \theta_x \end{aligned} \right\} \quad (3.1)$$

Step 2: Structural equations; the junctions structure i.e. 0-junctions and 1-junctions give the following equations from the causal bond graph structure relating efforts and flows:

$$\left. \begin{aligned} e_2 &= e_1 - e_3 - e_4 \\ e_3 &= t_1 e_5; e_4 = t_2 e_8 \\ e_{14} &= e_{13} + e_{12} \\ e_{12} &= t_3 e_{11} \\ f_{10} &= t_2 \dot{\beta} + t_3 \dot{\theta}_x \\ f_6 &= t_1 \dot{\beta} - f_{10} \\ e_5 &= e_6 = e_7 \\ e_8 &= e_9 = e_{11} \\ e_9 &= e_7 + e_{10} \end{aligned} \right\} \quad (3.2)$$

Step 3: Energy variables; these involved generation of the state equations for the ball-on-sphere system model. The independent energy-storage elements in preferential causality were used in the formulation of the system differential equations. Propagating

through the system causal bond graph structure, the following system equations were generated accordingly:

$$\begin{aligned}
e_2 &= e_1 - t_1 e_5 - t_2 e_8 \\
e_2 &= e_1 - t_1 B f_6 - t_2 e_9 \\
e_2 &= e_1 - t_1 B f_6 - t_2 (e_7 + e_{10}) \\
e_2 &= e_1 - t_1 B f_6 - t_2 \left(e_6 + I_b \dot{f}_{10} \right) \\
e_2 &= e_1 - t_1 B f_6 - t_2 \left(B f_6 + I_b \dot{f}_{10} \right)
\end{aligned} \tag{3.3}$$

$$e_2 + (t_1 + t_2) B f_6 + t_2 I_b \dot{f}_{10} = e_1 \tag{3.4}$$

But from the causal bond graph structure, e_2 and f_2 have the following relative equations:

$$\begin{aligned}
e_2 &= I_s \dot{f}_2 \\
f_2 &= \ddot{\beta}
\end{aligned}$$

Step 4: The System Dynamic Equations; the derived mathematical model of the ball-on-sphere system from the causal bond graph were obtained for the independent storage element (I_s) of bond 2.

Equation (3.4) results in:

$$I_s \ddot{\beta} + (t_1 + t_2) B \left(t_1 \dot{\beta} - \left(t_2 \dot{\beta} + t_3 \dot{\theta}_x \right) \right) + t_2 I_b \left(t_2 \ddot{\beta} + t_3 \ddot{\theta}_x \right) = \tau_y \tag{3.5}$$

Where, the transformation ratio t_1 , t_2 , and t_3 are defined as:

$$\begin{aligned}
t_1 &= \frac{R}{r} \\
t_2 &= \frac{R}{r} \\
t_3 &= \frac{(R + r)}{r}
\end{aligned}$$

From Figure 3.2, the transformation ratios, $T_1 = t_1$, $T_2 = t_2$ and $T_3 = t_3$.

Also, $e_3 = t_1 e_5$; $e_4 = t_2 e_8$

Equation (3.5) is simplified to equation (3.6)

$$\left[\frac{R(R+r)}{r^2} I_b \right] \ddot{\theta}_x + \left[I_s + \frac{R^2}{r^2} I_b \right] \ddot{\beta} - 2R \frac{(R+r)}{r^2} B \dot{\theta}_x = \tau_y \quad (3.6)$$

Similarly, from the causal bond graph structure of Figure 3.2, the equation generation procedures were repeated for the independent storage element (I_b) of bond 13:

$$\begin{aligned} e_{14} &= e_{13} + e_{12} \\ e_{12} &= t_3 e_{11} = t_3 e_9 \\ e_{14} &= e_{13} + t_3 e_9 \\ e_9 &= e_7 + e_{10} \\ e_{14} &= e_{13} + (e_7 + e_{10}) t_3 \\ e_{13} &= I' \dot{f}_{13}; e_7 = e_6 \\ I' \dot{f}_{13} + t_3 e_6 + t_3 e_{10} - e_{14} &= 0 \end{aligned} \quad (3.7)$$

$$I' \dot{f}_{13} + t_3 B \dot{f}_6 + t_3 I_b \dot{f}_{10} - e_{14} = 0 \quad (3.8)$$

But, from the causal bond graph structure, f_6 and f_{10} have the following relative equations:

$$f_6 = t_1 \dot{\beta} - f_{10}$$

$$f_{10} = t_2 \dot{\beta} + t_3 \dot{\theta}_x$$

$$I' \dot{f}_{13} + t_3 B \left(t_1 \dot{\beta} - (t_2 \dot{\beta} + t_3 \dot{\theta}_x) \right) + t_3 I_b (t_2 \ddot{\beta} + t_3 \ddot{\theta}_x) - mg \sin \theta_x = 0 \quad (3.9)$$

And $I' = m(R+r)^2$

Equation (3.9) is simplified to:

$$\left[(R+r)m + I_b \frac{(R+r)}{r^2} \right] \ddot{\theta}_x + \left[I_b \frac{R}{r^2} \right] \ddot{\beta} - \frac{(R+r)}{r^2} B \dot{\theta}_x - mg \sin \theta_x = 0 \quad (3.10)$$

Hence, the derived mathematical model of the ball-on-sphere system for the x-axis is described by:

$$\left[(R+r)m + I_b \frac{(R+r)}{r^2} \right] \ddot{\theta}_x + \left[I_b \frac{R}{r^2} \right] \ddot{\beta} - \frac{(R+r)}{r^2} B \dot{\theta}_x - mg \sin \theta_x = 0 \quad (3.11)$$

$$\left[\frac{R(R+r)}{r^2} I_b \right] \ddot{\theta}_x + \left[I_s + \frac{R^2}{r^2} I_b \right] \ddot{\beta} - 2R \frac{(R+r)}{r^2} B \dot{\theta}_x = \tau_y \quad (3.12)$$

Where τ_y is the torque exerted in y-axis direction, I_s is the moment of inertia of the sphere, R is the radius of the sphere, r is the radius of the ball and B is the frictional element.

However, the dynamic equations for the ball-and-sphere system in the x and y-axes are identical.

Hence, the corresponding equations for the y-axis are as shown:

$$\left[(R+r)m + I_b \frac{(R+r)}{r^2} \right] \ddot{\theta}_y + \left[I_b \frac{R}{r^2} \right] \ddot{\alpha} - \frac{(R+r)}{r^2} B \dot{\theta}_y - mg \sin \theta_y = 0 \quad (3.13)$$

$$\left[\frac{R(R+r)I_b}{r^2} \right] \ddot{\theta}_y + \left[I_s + \frac{R^2}{r^2} I_b \right] \ddot{\alpha} - \frac{2R(R+r)}{r^2} B \dot{\theta}_y = \tau_x \quad (3.14)$$

Equations (3.11), (3.12), (3.13) and (3.14) show the complete mathematical model of the ball-on-sphere system with double axis actuation (i.e. actuation on the x-and y-axes

respectively). Table 3.1 shows the parameters definition of the developed ball-on-sphere model.

Table 3.1: The Parameters Description of the System Model

Parameter	Description
R	Radius of the sphere
r	Radius of the ball
m	Mass of the ball
I_s	Moment of inertia of the sphere
I_b	Moment of inertia of the ball
B	Frictional parameter
g	gravitational acceleration
τ_x	Torque exerted in the x-axis direction
τ_y	Torque exerted in the y-axis direction
θ_x	Angular displacement of the ball relative to x-axis
θ_y	Angular displacement of the ball with respect to the y-axis
α	Angular displacement of the sphere with respect to y-axis
β	Angular displacement of the sphere with respect to x-axis

The developed mathematical model equations of the ball-on-sphere system were validated using 20-sim as shown in Figure 3.3.

```

20-sim Model Equations
static equations:
U1\p.e = U1\effort;

dynamic equations:
Js\p.f = Js\state / Js\j;
Jb\p.f = Jb\state / Jb\j;
Step\change = timeevent (Step\start_time);
Step\output = Step\amplitude * step (Step\start_time);
T1\p2.f = T1\gamma * Js\p.f;
T2\p2.f = T2\gamma * Js\p.f;
T3\p2.f = T3\gamma * Jb\p.f;
ZeroJunction\p2.f = T2\p2.f + T3\p2.f;
ZeroJunction1\p2.f = T1\p2.f + ZeroJunction\p2.f;
Ib\state = ZeroJunction\p2.f * Ib\j;
B\p.e = B\gamma * ZeroJunction1\p2.f;
T1\p1.e = T1\gamma * B\p.e;
Jb\p.e = (Step\output - T3\gamma * (B\p.e + ((T2\gamma * ((U1\p.e - (T2\gamma * B\p.e + T1\p1.e)) / Js\j)) * Ib\j)) / (1.0 + (T2\gamma * (T2\gamma / Js\j)) * Ib\j))) / (1.0 + T3\gamma * (((T3\gamma / Jb\j)) * Ib\j)) / (1.0 + (T2\gamma * (T2\gamma / Js\j)) * Ib\j));
Ib\p.e = ((T2\gamma * ((U1\p.e - (T2\gamma * B\p.e + T1\p1.e)) / Js\j) + T3\gamma * (Jb\p.e / Jb\j)) * Ib\j) / (1.0 + (T2\gamma * (T2\gamma / Js\j)) * Ib\j);
OneJunction1\p1.e = B\p.e + Ib\p.e;
T2\p1.e = T2\gamma * OneJunction1\p1.e;
T3\p1.e = T3\gamma * OneJunction1\p1.e;
Js\p.e = U1\p.e - (T2\p1.e + T1\p1.e);

system equations:
Js\state = int (Js\p.e, Js\state_initial);
Jb\state = int (Jb\p.e, Jb\state_initial);
OK

```

Figure 3.3: 20-Sim Model Equations for Ball-on-Sphere System

Figure 3.3 shows the 20-Sim program containing the system behavioural equations, systems dynamic equations, and the model equations of the ball-on-sphere used for validation.

3.3.3.1 Behavioural equations

In the 20-Sim program, the system bond graph elements are associated with its underlying physical characteristic equations. These basic constitutive equations are known as the behavioural equations of the elements. The physical laws expressing how the energy is transformed are mathematically described by the behaviour model. For the ball-on-sphere system, the behavioural equations obtained are as follows:

$$I : J_s \rightarrow f_2 = \frac{1}{J_s} \int e_2 dt \quad (3.15)$$

$$I : J_b \rightarrow f_{13} = \frac{1}{J_b} \int e_{13} dt \quad (3.16)$$

$$I : I_b \rightarrow e_{10} = I_b \frac{df_{10}}{dt} \quad (3.17)$$

$$R : B \rightarrow e_1 = f_6 \quad (3.18)$$

$$Se : u_1 \rightarrow e_1 = \tau_y \quad (3.19)$$

$$MSe : u_2 \rightarrow f_{13} = \frac{1}{m(R+r)^2} \int e_{13} dt \quad (3.20)$$

Where the J_s is the moment inertia of the sphere, J_b and I_b are the moment of inertia due to the ball rotating and revolving round the sphere respectively, B is the frictional parameter and u_1 and u_2 are sources of effort.

3.3.3.2 System dynamics

The ball-on-sphere system dynamics is an approach to understanding the behaviour of the system over time. It deals with internal feedback loops and time delays that affect the behaviour of the whole system. Thus, the interconnections between the system elements are derived as follows:

$$J_s \backslash p.f = J_s \backslash state / J_s \backslash i \quad (3.21)$$

$$J_b \backslash p.f = J_b \backslash state / J_b \backslash i \quad (3.22)$$

Where the J_s is the moment inertia of the sphere and J_b is the moment of inertia of the ball.

3.3.3.3 System equations

The ball-on-sphere system equations describe the whole characteristics of the modeled physical system. These are derived as follows:

$$J_s \backslash \text{state} = \int (J_s \backslash p.e, J_s \backslash \text{state_initial}) \quad (3.23)$$

$$J_b \backslash \text{state} = \int (J_b \backslash p.e, J_b \backslash \text{state_initial}) \quad (3.24)$$

3.3.4 Ball-on-Sphere Bond Graph Subcomponents

The detailed dynamic information of the segmented parts of the ball-on-sphere system bond graph structure when divided into subcomponents is depicted in Figures 3.4 and 3.5. These figures show the physical quantities of the segmented ball-on-sphere system.

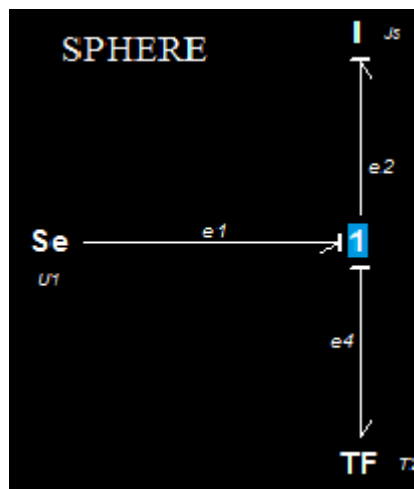


Figure 3.4: Sphere Dynamic Information

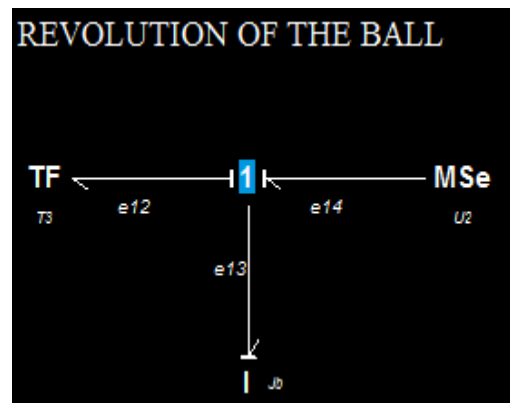
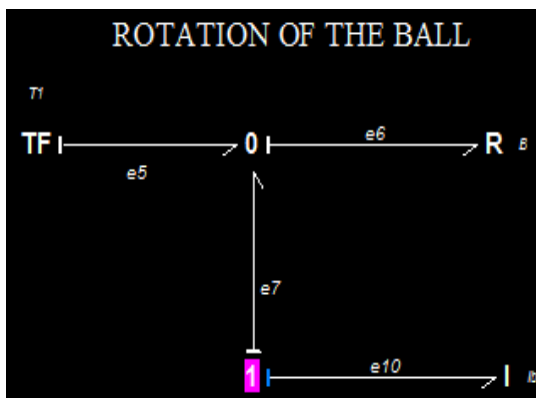


Figure 3.5: Rotational and Translational Ball Dynamics

From Figure 3.4 and Figure 3.5, the system variables and structural equations are defined as follows:

Variables

The vector, V contains all power bond variables i.e. product of effort (e) and flow (f) as deduced from the bond graph structure of Figures 3.4 and 3.5:

$$V = [e_1 f_1, e_2 f_2, e_6 f_6, e_{10} f_{10}, e_{13} f_{13}, e_{14} f_{14}] \quad (3.25)$$

This results in the total number of six (6) components.

Structural Equations

From the segmented ball-on-sphere system of Figures 3.4 and Figure 3.5 the structural equations are derived for both the components connected to the 1-junctions and 0-junction respectively as:

1) 1-junctions:

Let J represents junction.

$$J1: e_2 = e_1 - e_3 - e_4 \quad (3.26)$$

$$J2: e_9 = e_7 + e_{10} \quad (3.27)$$

$$J3: e_{14} = e_{13} + e_{12} \quad (3.28)$$

2) 0-junctions:

$$J4: f_7 = f_6 - f_5 \quad (3.29)$$

$$J5: f_8 = f_9 - f_{11} \quad (3.30)$$

a. Transformers:

$$J6: e_3 = t_1 e_5 \quad (3.31)$$

Where;

$$t_1 = \frac{R}{r}$$

$$J7: e_4 = t_2 e_8 \quad (3.32)$$

Where;

$$t_2 = \frac{R}{r}$$

$$J8: e_{12} = t_3 e_{11} \quad (3.33)$$

Where;

$$t_3 = \frac{(R+r)}{r}$$

3.3.5 Simulink Model of the Ball-on-Sphere System

The Simulink which forms the core environment for model-based design for creating accurate mathematical models of physical system was used for the design of the ball-on-sphere system in order to appreciate the contribution of each modeled effect to the dynamics of the system.

The developed mathematical model of the ball-on-sphere system with frictional effects is as shown:

$$\left[(R+r)m + I_b \frac{(R+r)}{r^2} \right] \ddot{\theta}_x + \left[I_b \frac{R}{r^2} \right] \ddot{\beta} - \frac{(R+r)}{r^2} B \dot{\theta}_x - mg \sin \theta_x = 0 \quad (3.34)$$

$$\left[\frac{R(R+r)}{r^2} I_b \right] \ddot{\theta}_x + \left[I_s + \frac{R^2}{r^2} I_b \right] \ddot{\beta} - 2R \frac{(R+r)}{r^2} B \dot{\theta}_x = \tau_y \quad (3.35)$$

$$\left[(R+r)m + I_b \frac{(R+r)}{r^2} \right] \ddot{\theta}_y + \left[I_b \frac{R}{r^2} \right] \ddot{\alpha} - \frac{(R+r)}{r^2} B \dot{\theta}_y - mg \sin \theta_y = 0 \quad (3.36)$$

$$\left[\frac{R(R+r)I_b}{r^2} \right] \ddot{\theta}_y + \left[I_s + \frac{R^2}{r^2} I_b \right] \ddot{\alpha} - \frac{2R(R+r)}{r^2} B \dot{\theta}_y = \tau_x \quad (3.37)$$

In order to simplify equation (3.36) and (3.37), the following assumptions were made:

Let

$$a \ddot{\theta}_x + b \ddot{\beta}_x - c \dot{\theta}_x - mg \sin \theta_x = 0 \quad (3.38)$$

$$d\ddot{\theta}_x + e\ddot{\beta}_x - f\dot{\theta}_x = \tau_y \quad (3.39)$$

$$s\ddot{\theta}_y + t\ddot{\beta}_y - u\dot{\theta}_y - mg \sin \theta_y = 0 \quad (3.40)$$

$$v\ddot{\theta}_y + w\ddot{\beta}_y - x\dot{\theta}_y = \tau_x \quad (3.41)$$

Where

$$a = (R+r)m + I_b (R+r) / r^2$$

$$b = I_b R / r^2$$

$$c = \frac{(R+r)}{r^2} B$$

$$d = I_b (R+r) / r^2$$

$$e = I_B + I_b (R/r)^2$$

$$f = 2R \frac{(R+r)}{r^2} B$$

$$p = a - (b*d) / e;$$

$$q = b - (a*e) / d$$

$$a = s; b = t; c = u; d = v; e = w; f = x;$$

And let

$$\phi = \frac{e}{ae - bd}, \theta = \frac{d}{bd - ae}, \psi = \frac{w}{sw - tv}, \gamma = \frac{v}{tv - sw},$$

$$A = \frac{ec - bf}{e}, B = \frac{cd - af}{d}, Y = \frac{uw - tx}{w}, Z = \frac{uv - sx}{v}$$

$$\ddot{\theta}_x = mg\phi \sin \theta_x + A\dot{\theta}_x - \frac{b\phi}{e} \tau_y \quad (3.42)$$

$$\ddot{\beta}_x = mg\theta \sin \theta_x + B\dot{\theta}_x - \frac{a\theta}{d} \tau_y \quad (3.43)$$

$$\ddot{\theta}_y = mg\psi \sin \theta_y + Y\psi \dot{\theta}_y - \frac{t\psi}{w} \tau_x \quad (3.44)$$

$$\ddot{\beta}_y = mg\gamma \sin \theta_y + Z\gamma \dot{\theta}_y - \frac{s\gamma}{v} \tau_x \quad (3.45)$$

With the change of coordinates, these become:

$$\dot{x}_1 = \dot{x}_5 = \dot{\theta}_x$$

$$\dot{x}_2 = \dot{x}_6 = \dot{\beta}_x$$

$$\dot{x}_3 = \dot{x}_7 = \dot{\theta}_y$$

$$\dot{x}_4 = \dot{x}_8 = \dot{\beta}_y$$

$$\dot{x}_5 = \ddot{\theta}_x = mg\phi \sin \theta_x + A\phi \dot{\theta}_x - \frac{b\phi}{e} \tau_y$$

$$\dot{x}_6 = \ddot{\beta}_x = mg\theta \sin \theta_x + B\theta \dot{\theta}_x - \frac{a\theta}{d} \tau_y$$

$$\dot{x}_7 = \ddot{\theta}_y = mg\psi \sin \theta_y + Y\psi \dot{\theta}_y - \frac{t\psi}{w} \tau_x$$

$$\dot{x}_8 = \ddot{\beta}_y = mg\gamma \sin \theta_y + Z\gamma \dot{\theta}_y - \frac{s\gamma}{v} \tau_x$$

The dynamic equations after augmenting with the terms for torque become:

$$\ddot{\theta}_x = mg\phi \sin x_1 + \frac{b\phi}{e} \left(\frac{R}{d_m} \right)^2 \frac{K_m}{R_a} x_5 - \frac{b\phi}{e} \frac{R}{d_m} \frac{K_m}{R_a} u_1 + A\phi x_5 \quad (3.46)$$

$$\ddot{\beta}_x = mg\theta \sin x_1 + \frac{a\theta}{d} \left(\frac{R}{d_m} \right)^2 \frac{K_m}{R_a} x_5 - \frac{a\theta}{d} \frac{R}{d_m} \frac{K_m}{R_a} u_1 + B\theta x_5 \quad (3.47)$$

$$\ddot{\theta}_y = mg\psi \sin x_3 + \frac{T\psi}{w} \left(\frac{R}{d_m} \right)^2 \frac{K_m}{R_a} x_5 - \frac{T\psi}{w} \frac{R}{d_m} \frac{K_m}{R_a} u_2 + Y\psi x_5 \quad (3.48)$$

$$\ddot{\beta}_y = mg\gamma \sin x_3 + \frac{s\gamma}{v} \left(\frac{R}{d_m} \right)^2 \frac{K_m}{R_a} x_5 - \frac{s\gamma}{v} \frac{R}{d_m} \frac{K_m}{R_a} u_2 + Z\gamma x_5 \quad (3.49)$$

The Simulink model of the developed mathematical model of ball-on-sphere system is shown in Figure 3.6.

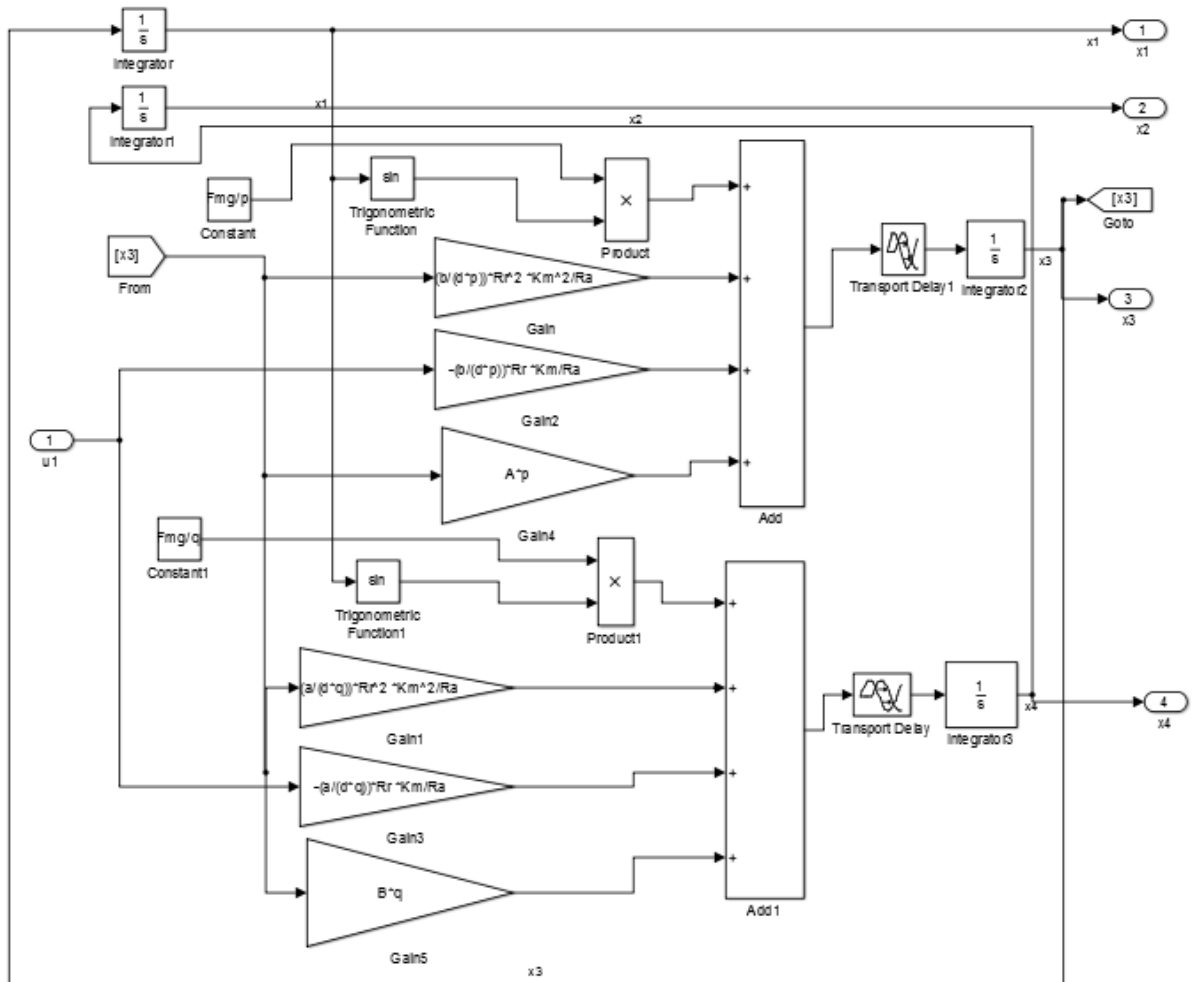


Figure3.6: Simulink Model of the Ball-on-Sphere System

3.4 20-SIM VALIDATION OF BOND-ON-SPHERE SYSTEM MODEL

These steps explain the procedures used in validating the developed bond graph model of the ball-on-sphere system using the 20-Sim software. In the validation process:

- 1) The ball-on-sphere systems physical components were first identified from the 20-Sim bond graph library.
- 2) The identified components were used in building the ball-on-sphere system model and power bonds were assigned to the connected components.

- 3) The 20-sim graphical interface has the capacity to automatically assign causalities, as such, the connected power bonds were appropriately assigned causalities in order to verify the causalities assigned to the developed analytical model of the ball-on-sphere system.
- 4) The 20-sim was used to process and diagnose the developed model to ensure the model is error free.

3.5 STRUCTURAL ANALYSIS OF THE BALL-ON-SPHERE SYSTEM

The bond graph structural analysis technique for the developed causal bond graph model of the ball-on-sphere system are presented. The structural analysis carried out on the system include; structural controllability, structural observability, inverse model analysis and input-output decoupling analysis of the system.

3.5.1 Ball-on-Sphere System Structural Controllability Analysis

The steps of the bond graph structural analysis approach used in determining the structural controllability test on the developed causal bond graph model of the ball-on-sphere system are explained.

The ball-on-sphere system satisfied the bond graph structural controllability analysis two conditions:

- 1) In the bond graph model, there is a causal path ($e_1 - e_2$) connecting the storage element of the sphere i.e. the moment of inertia of the sphere (I:Js) in preferential integral causality and the control source (Se). Similarly, there exist a causal path ($e_{14} - e_{13}$) between the storage element of the ball i.e. the moment of inertia of the ball (I:Jb) in preferential causality and the source (MSe). The causal paths connecting the Source and Storage element of the ball-on-sphere system is shown in Figure 3.7

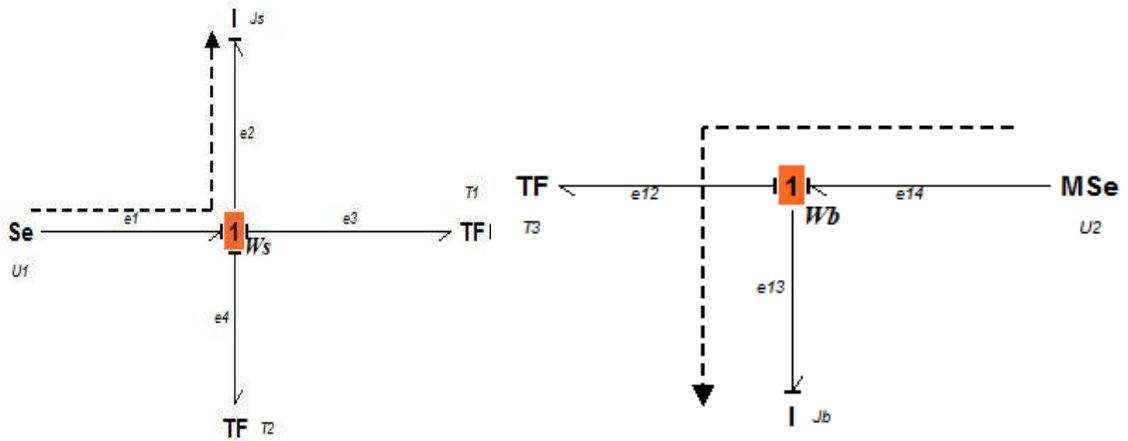


Figure 3.7: Causal Path of Source and Storage elements for Controllability Analysis

- 2) The storage element of the sphere (I:Js) and the storage element of the ball (I:Jb) in preferential integral causalities respectively accept a preferential derivative causalities without violating the ball-on-sphere system causalities norms. The storage elements with assigned derivative causalities are shown in Figure 3.8

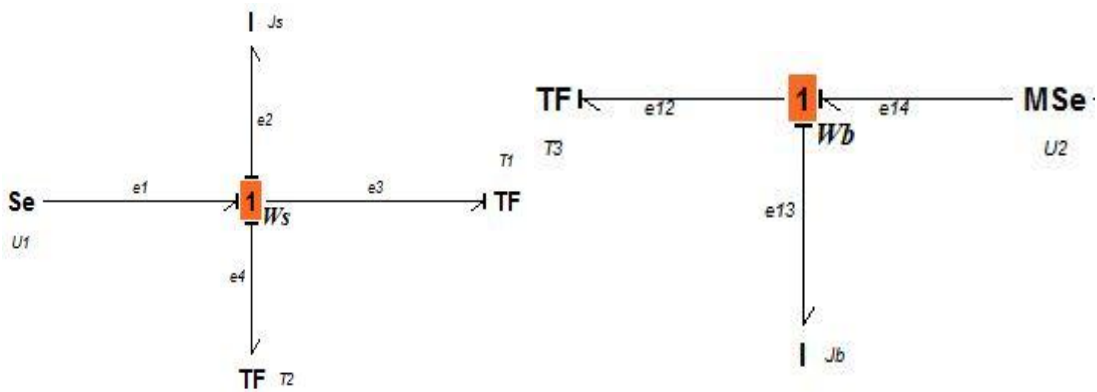


Figure 3.8: Derivative Storage Elements for Controllability Analysis

3.5.2 Ball-on-Sphere System Structural Observability Analysis

The bond graph structural analysis method used in determining the structural observability test on the developed causal bond graph model of the ball-on-sphere system is explained in this subsection.

The ball-on-sphere system satisfied the bond graph structural observability analysis on two conditions:

- 1) In the bond graph model, there exist a causal path ($f_2 - D_f$) linking the storage element i.e. the moment of inertia of the sphere (I:Js) in the preferential integral causality and the flow detector (Df) introduced to detect the output i.e. the angular velocity of the sphere (Ws). Similarly, there exist a causal path ($f_{13} - D_f$) connecting the storage element of the ball i.e. the moment of inertia of the ball (I:Jb) in preferential causality and the flow detector (Df) introduced to detect the output i.e. the angular velocity of the ball (Wb). The causal paths connecting the Source and detector of the ball-on-sphere system is shown in Figure 3.9

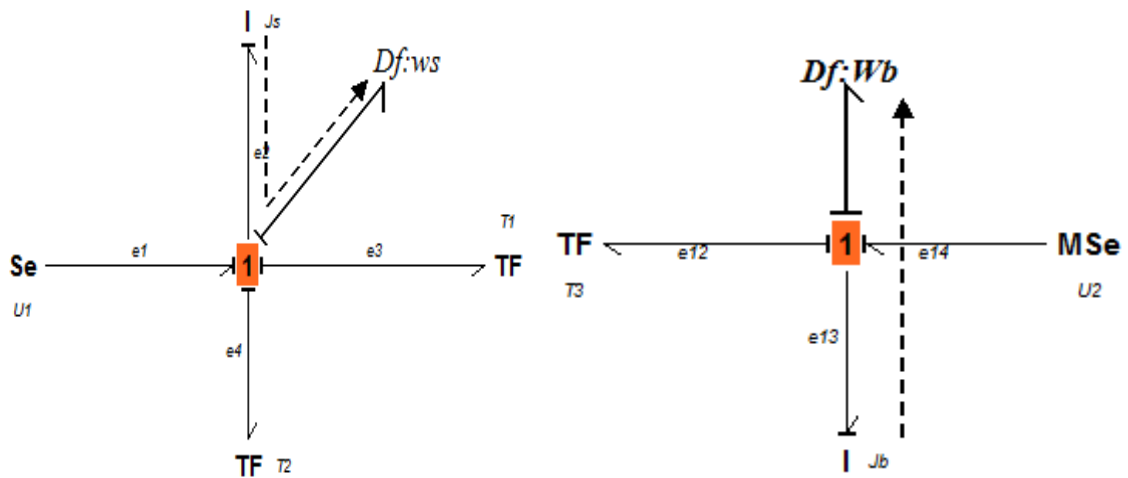


Figure 3.9: Causal Path Connecting Storage Elements and Detector for Observability Analysis

- 2) The storage element of the sphere i.e. the moment of inertia of the sphere (I:Js) and the storage element of the ball i.e. the moment of inertia of the ball (I:Jb) in preferential integral causalities respectively accept preferential derivative causalities without violating the ball-on-sphere system causalities norms. The storage elements with assigned derivative causalities are shown in Figure 3.10

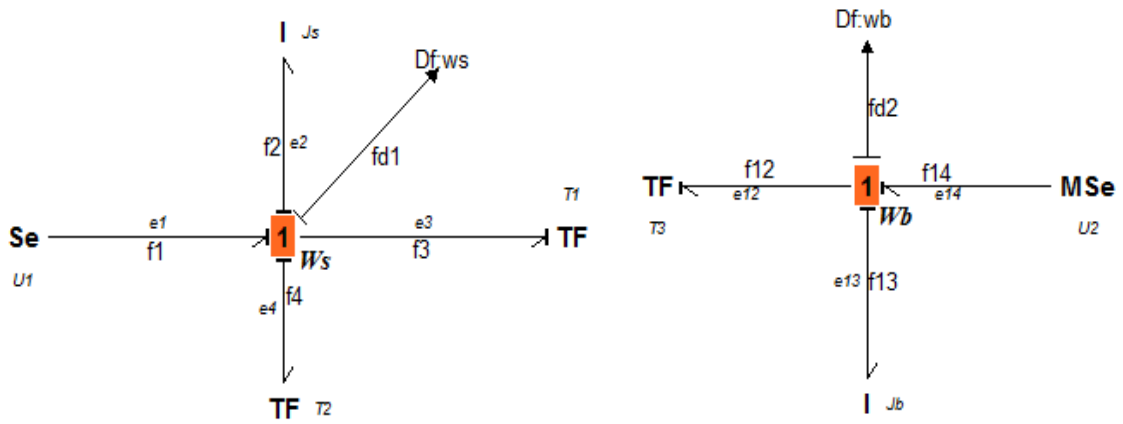


Figure 3.10: Derivative Storage Elements for Observability Analysis

3.5.3 Ball-on-Sphere System Inverse Model Analysis

The bond graph procedures involved in determining the inverse model of the ball-on-sphere system are explain in this subsection.

The following steps explain the process involved in the inverse model representation of the system:

- 1) Independent input-output power lines test was performed on the ball-on-sphere system bond graph model. The system has two independent input-output power lines, (u_1, y_1) and (u_2, y_2) .
- 2) In the developed causal bond graph model of the ball-on-sphere system, the system has two disjoint input-output causal paths on the ball-on-sphere system bond graph model. Figure 3.11 presents the disjoint input-output causal paths. These are (u_1, y_1) :

$$e_1 - e_2 - f_2 - f_{d1} \text{ and } (u_2, y_2) : e_{14} - e_{13} - f_{13} - f_{d2}.$$

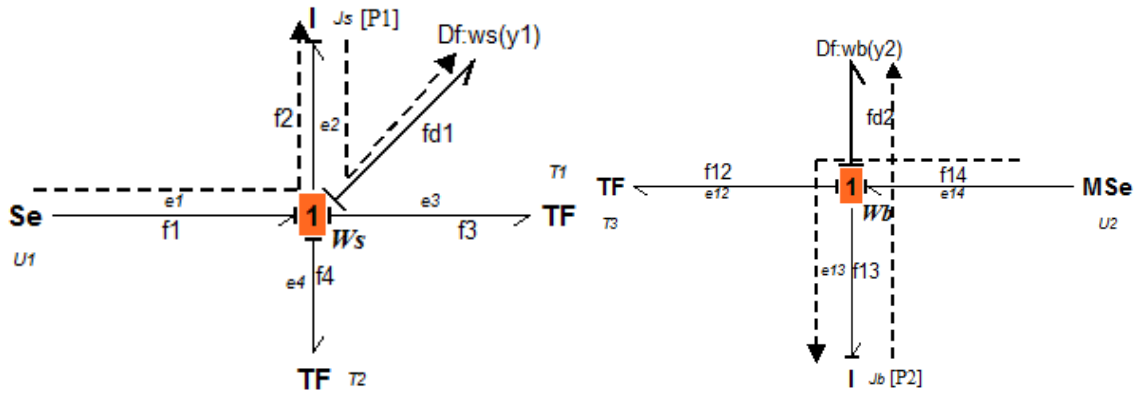


Figure 3.11 Disjoints Input-Output Causal Path for Invertibility Analysis

- 3) Steps 1) and 2) satisfied the invertibility test condition of the ball-on-sphere system.
- 4) The bi-causality assignment procedure was thus used to obtain the inverse model of the ball-on-sphere system. The sources (Se:u1 and MSe:u2) and the detectors (Df:y1 and Df:y2) in Figure 3.11 were respectively replaced by double source (SeSf:y1 and SeSf:y2) and double detector (DeDf:u1 and DeDf:u2) as shown in Figure 3.12. Bi-causality was used to propagate both effort and flow variables in the system.

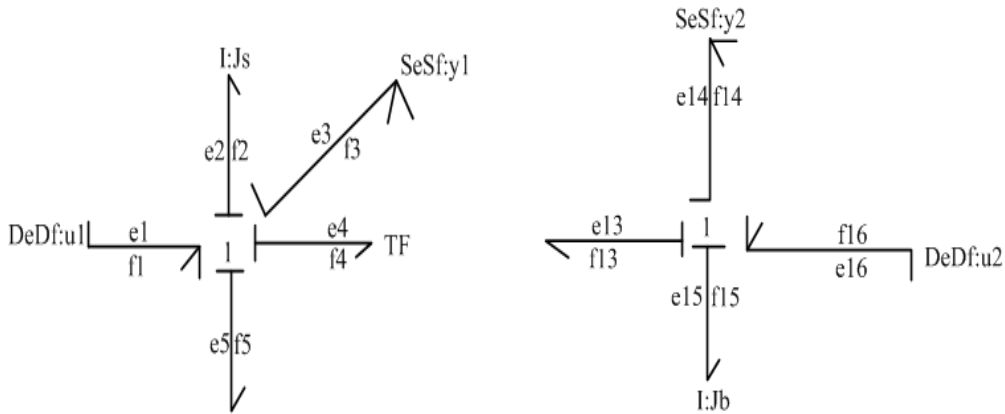


Figure 3.12: Bicausality for Ball-on-Sphere Inverse Model

- 5) The bi-causality propagation using the sequential causality assignment procedures for inversion (SCAPI) and the causality propagation using the sequential causality assignment procedure (SCAP) were performed on the ball-on-sphere system inverse model.

3.5.4 Ball-on-Sphere System Input-Output Decoupling Analysis

The steps of the input-output analysis of the ball-on-sphere system bond graph model are presented.

These steps explain the input-output decoupling process of the system:

- 1) The state ($x = [p_1 p_2]^T$), input ($u = [u_1 u_2]^T$) and output ($y = [y_1 y_2]^T$) vectors of the ball-on-sphere system were determined from the system causal bond graph model.
- 2) The lengths of disjoint causal paths were calculated from the disjoint input-output causal paths of the ball-on-sphere system bond graph model using the storage elements in integral causality along the causal paths.
- 3) From the length of the causal paths, the decoupling of the ball-on-sphere system was determined.

3.6 State Space Generation of the Ball-on-Sphere Model

The developed nonlinear dynamical equations of the ball-on-sphere system with double axis actuation (i.e. actuation on the x-and y-axes respectively) are as shown:

$$\left[(R+r)m + I_b \frac{(R+r)}{r^2} \right] \ddot{\theta}_x + \left[I_b \frac{R}{r^2} \right] \ddot{\beta} - \frac{(R+r)}{r^2} B \ddot{\theta}_x - mg \sin \theta_x = 0 \quad (3.50)$$

But, $\sin \theta_x = \theta_x$

$$\left[(R+r)m + I_b \frac{(R+r)}{r^2} \right] \ddot{\theta}_x + \left[I_b \frac{R}{r^2} \right] \ddot{\beta} - \frac{(R+r)}{r^2} B \ddot{\theta}_x - mg \theta_x = 0 \quad (3.51)$$

$$\left[\frac{R(R+r)}{r^2} I_b \right] \ddot{\theta}_x + \left[I_s + \frac{R^2}{r^2} I_b \right] \ddot{\beta} - 2R \frac{(R+r)}{r^2} B \ddot{\theta}_x = \tau_y \quad (3.52)$$

$$\left[(R+r)m + I_b \frac{(R+r)}{r^2} \right] \ddot{\theta}_y + \left[I_b \frac{R}{r^2} \right] \ddot{\alpha} - \frac{(R+r)}{r^2} B \ddot{\theta}_y - mg \sin \theta_y = 0 \quad (3.53)$$

But, $\sin \theta_y = \theta_y$

$$\left[(R+r)m + I_b \frac{(R+r)}{r^2} \right] \ddot{\theta}_y + \left[I_b \frac{R}{r^2} \right] \ddot{\alpha} - \frac{(R+r)}{r^2} B \dot{\theta}_y - mg \theta_y = 0 \quad (3.54)$$

$$\left[\frac{R(R+r)I_b}{r^2} \right] \ddot{\theta}_y + \left[I_s + \frac{R^2}{r^2} I_b \right] \ddot{\alpha} - \frac{2R(R+r)}{r^2} B \dot{\theta}_y = \tau_x \quad (3.55)$$

The nonlinear terms were linearized about an operating point i.e. at angular displacement ($\theta = 0$). Hence, $\sin \theta = \theta$ in order to obtain an approximate linear state space model for numerical analysis.

The resulted approximate linear equations of the ball-on-sphere system are transformed to obtain state space transformation analysis of the system.

$$q = [\theta_x \quad \beta \quad \theta_y \quad \alpha]$$

Where q is the generalized coordinate.

The dynamical model of the ball-on-sphere system is stated in the form of matrices as shown:

$$M \ddot{q} + B \dot{q} = T \quad (3.56)$$

$$\ddot{q} = M^{-1}(T - B \dot{q})$$

The approximate linear model of equations (3.51), (3.52), (3.54) and (3.55) were transformed into state space form:

$$x_1 = \theta_x; x_2 = \dot{\theta}_x$$

$$x_3 = \beta; x_4 = \dot{\beta}$$

$$x_5 = \theta_y; x_6 = \dot{\theta}_y$$

$$x_7 = \alpha; x_8 = \dot{\alpha}$$

\therefore

$$\begin{aligned}
x_1 &= x_2; x_2 = \theta_x \\
x_3 &= x_4; x_4 = \beta \\
x_5 &= x_6; x_6 = \theta_y \\
x_7 &= x_8; x_8 = \alpha
\end{aligned}$$

$$\begin{pmatrix} M_{11} & M_{12} \\ M_{21} & M_{22} \end{pmatrix} \begin{pmatrix} X_{11} \\ X_{21} \end{pmatrix} = \begin{pmatrix} A_{11} & A_{12} \\ A_{21} & A_{22} \end{pmatrix} \begin{pmatrix} X_{11} \\ X_{21} \end{pmatrix} + \begin{pmatrix} B_{11} & B_{12} \\ B_{21} & B_{22} \end{pmatrix} \begin{pmatrix} T_1 \\ T_2 \end{pmatrix}$$

$$M_{11} = M_{22} = \begin{pmatrix} 1 & 0 & 0 & 0 \\ 0 & a_1 & 0 & a_2 \\ 0 & 0 & 1 & 0 \\ 0 & a_5 & 0 & a_6 \end{pmatrix}; M_{12} = M_{21} = \begin{pmatrix} 0 & 0 & 0 & 0 \\ 0 & 0 & 0 & 0 \\ 0 & 0 & 0 & 0 \\ 0 & 0 & 0 & 0 \end{pmatrix}; X_{11} = \begin{pmatrix} x_1 \\ x_2 \\ x_3 \\ x_4 \end{pmatrix}; X_{21} = \begin{pmatrix} x_5 \\ x_6 \\ x_7 \\ x_8 \end{pmatrix};$$

$$A_{11} = A_{22} = \begin{pmatrix} 0 & 1 & 0 & 0 \\ -a_4 & -a_3 & 0 & 0 \\ 0 & 0 & 0 & 1 \\ 0 & -a_7 + b_2 & 0 & 0 \end{pmatrix}; A_{21} = A_{12} = \begin{pmatrix} 0 & 0 & 0 & 0 \\ 0 & 0 & 0 & 0 \\ 0 & 0 & 0 & 0 \\ 0 & 0 & 0 & 0 \end{pmatrix}; X_{11} = \begin{pmatrix} X_1 \\ X_2 \\ X_3 \\ X_4 \end{pmatrix}$$

$$; X_{21} = \begin{pmatrix} X_5 \\ X_6 \\ X_7 \\ X_8 \end{pmatrix}$$

$$B_{11} = B_{22} = \begin{pmatrix} 0 \\ 0 \\ 0 \\ b_1 \end{pmatrix}; B_{21} = B_{12} = \begin{pmatrix} 0 \\ 0 \\ 0 \\ 0 \end{pmatrix}; T_1 = \begin{pmatrix} 0 \\ \tau_x \end{pmatrix}; T_2 = \begin{pmatrix} 0 \\ \tau_y \end{pmatrix}$$

Where

$$a_1 = (R+r)m + I_b \frac{(R+r)}{r^2} ; \quad a_2 = I_b \frac{R}{r^2} ; \quad a_3 = -\frac{(R+r)}{r^2} B ; \quad a_4 = -mg ;$$

$$a_5 = I_b \frac{R(R+r)}{r^2} ; a_6 = I_s + \frac{R^2}{r^2} I_b ; \quad a_7 = -\frac{2R(R+r)B}{r^2} ; \quad b1 = R / d * K_b / R_a ;$$

$$b2 = -R_a * b1^2 .$$

The generated matrices were used in the numerical analysis of the ball on sphere system control test solution. The numerical approach depends on the physical parameters values of the system as defined in table 3.2.

Table 3.2: The Physical Parameters of the System (Liu *et al.*, 2011)

Parameter	Description	Value (Units)
R	Radius of the sphere	0.099 (m)
r	Radius of the ball	0.011 (m)
M	Mass of the ball	0.012 (kg)
I_s	Moment of inertia of the sphere	5.808×10^{-7} (kgm ²)
I_b	Moment of inertia of the ball	0.99 (kgm ²)
G	Gravitational acceleration	9.8 (m/sec ²)
B	Frictional Parameter	1.6885×10^{-5}
d	Radius of the friction wheel	0.032 (m)
R_a	Motor armature resistance	0.6510 (Ω)
K_b	Motor constant	0.643 -m/A)

3.7 Matrix Approach of Invertibility and Decoupling of Ball-on-Sphere System

This section explains the procedures of inverse and decoupling analysis of the ball-on-sphere system using matrix numerical algebraic approach.

The generated matrices of the ball-on-sphere system (A, B and C) were used in the analyses.

$$A_{11} = A_{22} = \begin{pmatrix} 0 & 1 & 0 & 0 \\ -a_4 & -a_3 & 0 & 0 \\ 0 & 0 & 0 & 1 \\ 0 & -a_7 + b_2 & 0 & 0 \end{pmatrix}; A_{21} = A_{12} = \begin{pmatrix} 0 & 0 & 0 & 0 \\ 0 & 0 & 0 & 0 \\ 0 & 0 & 0 & 0 \\ 0 & 0 & 0 & 0 \end{pmatrix}; \quad A = \begin{pmatrix} A_{11} & A_{12} \\ A_{21} & A_{22} \end{pmatrix};$$

$$B_{11} = B_{22} = \begin{pmatrix} 0 \\ 0 \\ 0 \\ b_1 \end{pmatrix}; B_{21} = B_{12} = \begin{pmatrix} 0 \\ 0 \\ 0 \\ 0 \end{pmatrix}; B = \begin{pmatrix} B_{11} & B_{12} \\ B_{21} & B_{22} \end{pmatrix}$$

$$C_{11} = C_{22} = \begin{pmatrix} 1 & 0 & 0 & 0 \\ 0 & 1 & 0 & 0 \\ 0 & 0 & 1 & 0 \\ 0 & 0 & 0 & 1 \end{pmatrix}; C_{21} = C_{12} = \begin{pmatrix} 0 & 0 & 0 & 0 \\ 0 & 0 & 0 & 0 \\ 0 & 0 & 0 & 0 \\ 0 & 0 & 0 & 0 \end{pmatrix}; C = \begin{pmatrix} C_{11} & C_{12} \\ C_{21} & C_{22} \end{pmatrix}$$

.

The ball-on-sphere system state space is described by:

$$\begin{aligned} \dot{x} &= Ax + Bu \\ y &= Cx \end{aligned} \tag{3.57}$$

Where $x \in R^n$, $u \in R^p$, and $y \in R^p$ are respectively the state, input and output vectors of the system. The inverse model is obtained from the direct model (3.57) of the ball-on-sphere system.

The ball-on-sphere system (3.57) is full column rank, with a transfer function matrix $T(s)$ strictly proper and defined by:

$$T(s) = C(sI - A)^{-1}B = \begin{pmatrix} 0 & 0 \\ 0 & 0 \\ \frac{0.3056}{s^2} & 0 \\ 0 & 0 \\ 0 & 0 \\ 0 & \frac{0.3056}{s^2} \\ 0 & \frac{0.3056}{s} \end{pmatrix}.$$

The Matlab codes used for computing the transfer function matrix $T(s)$ for the invertibility analysis of the ball-on-sphere system are presented in Appendix B. From the analysis, the ball-on-sphere system contains two (2) infinite zeros order i.e. $p=2$, hence the system is invertible.

In the decoupling analysis, the rank of $T(s)$ is equal to p and $T(s)$ at infinity is the unique matrix $\Phi(s)$ defined by equation:

$T(s) = B_1(s)\Phi(s)B_2(s)$, where $B_1(s)$ and $B_2(s)$ are biproper i.e. proper rational matrix with proper inverse and $\Phi(s) = \text{diag}(s^{-n_1}, \dots, s^{-n_p})$. From the ball-on-sphere system transfer function $T(s)$, the row and global infinite and unstable zeros of the system coincides, and thus the system is decouplable with stability.

CHAPTER FOUR

RESULTS AND DISCUSSION

4.1 INTRODUCTION

The results obtained in this work are presented and discussed in this chapter. These include the bond graph model of the ball-on-sphere system and the mathematical model of the system derived from the developed causal bond graph. The results of the bond graph structural analysis of the developed model are also presented and discussed.

4.2 BALL-ON-SPHERE SYSTEM MODEL

The developed bond graph model without causality, the causal bond graph and the derived mathematical model of the ball-on-sphere system are presented and discuss as follows.

4.2.1 Bond Graph Model of Ball-on-Sphere System

The developed bond graph model of the ball-on-sphere system is as shown in Figure 4.1. The bond graph graphical representation of the system shows the dynamics of the rotation and revolution of the ball as the sphere rotates due to the applied torque. The developed bond graph model is without causal assignment. This means there is no causal and effect relationship specified in the model and as such, no further analysis can be carried out on the developed model such as deriving the mathematical model of the ball-on-sphere system and amongst other.

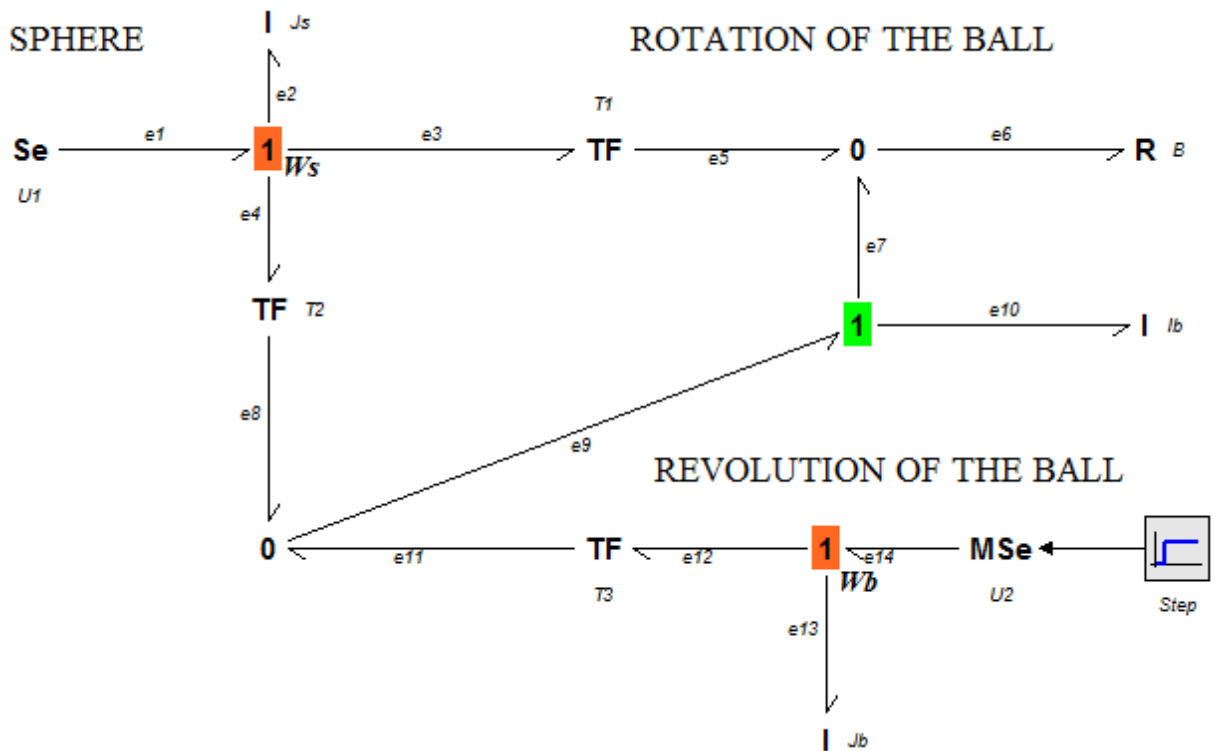


Figure 4.1: Bond Graph Model of Ball-on-Sphere System Without Causality

4.2.2 Bond Graph Causal Model of Ball-on-Sphere System

Causality were assigned to the developed bond graph model of the ball-on-sphere system based on the sequential causality assignment procedures (SCAP) as shown in Figure 4.2. The developed causal bond graph model shows the cause and effect relationship in the system and also specifies the transfer of energy within the system. From the developed causal bond graph model, further analyses such as mathematical model and structural analysis can be deduced in order to study the dynamic behaviour of the system.

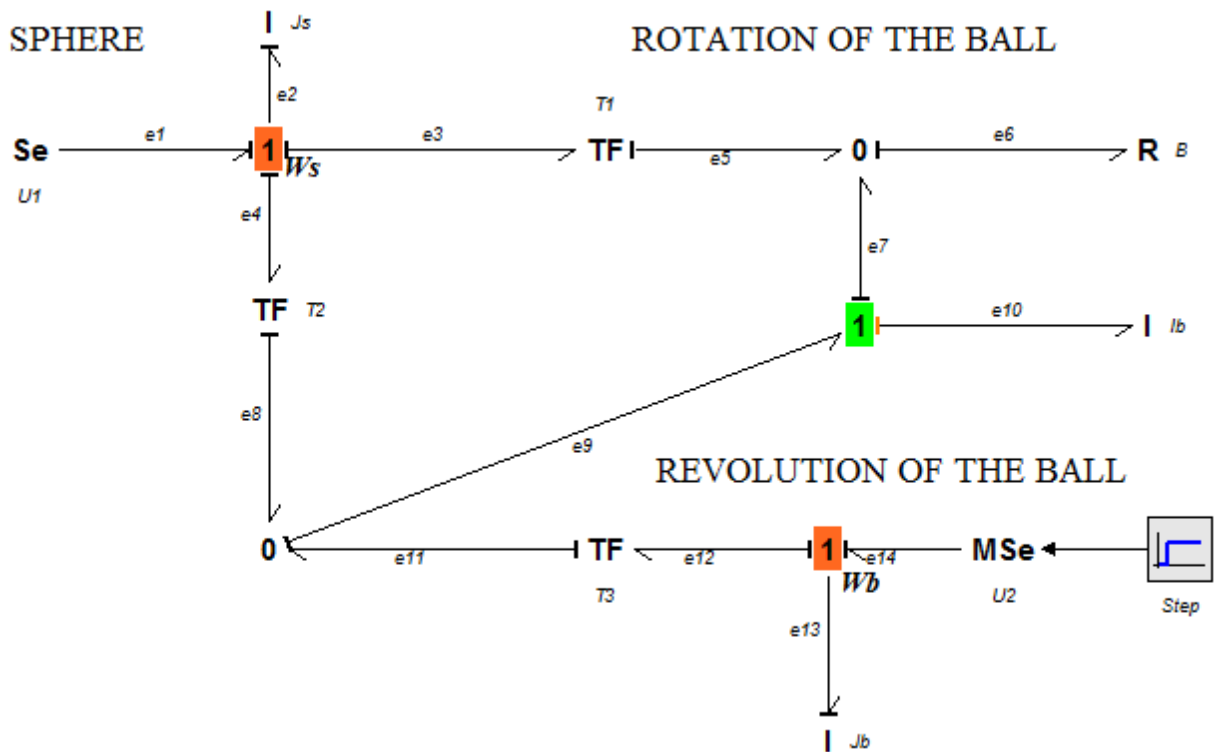


Figure 4.2: Causal Bond Graph of Ball-on-Sphere System

It can be observed from the causal bond graph model of Figure 4.2 that:

- 1) The source of energy elements satisfied the required causality assignment with an effort source (Se).
- 2) The two-port elements and multi-port junctions i.e. the 0-junctions,1-junctions and transformers satisfied the restricted causality assignment without violating the junctions causality norms.
 - a) At 0-junctions, there is constant effort, as such, only one element can set the effort propagation and also,only one causal stroke will be assigned near the 0-junction structures.
 - b) At 1-junctions, there is constant flow, as such, only one element can set the flow propagation and all the causal stroke will be assigned near the 1-junction structures except one causal stroke.

- c) At transformer (TF) port, effort and flow at one port determines effort and flow at the other and only one causal stroke is assigned near the TF.
- 3) The independent energy-storage elements (I_s and I_b) were assigned integral causality
- 4) The dependent energy-storage element (I_b) was assigned derivative causality and
- 5) The resistive element (B) was assigned arbitrary causality which was determined by the rest of the system.

4.2.3 Mathematical Model of Ball-on-Sphere System

The mathematical equations obtained from the causal bond graph of the ball-on-sphere system model describe the dynamics of the ball-on-sphere system with respect to the integrals of the storage elements which are the state variables of the system. All the integral storage elements i.e. moment of inertia of the ball and sphere i.e. (I_s and I_b) correspond to stored state variables (P i.e. momentum) and equations were derived for their time derivatives (i.e. effort and flow).

The dynamic equations for the ball-on-sphere system in the x and y-axes are identical.

Hence, the corresponding equations are as shown:

$$\left[(R+r)m + I_b \frac{(R+r)}{r^2} \right] \ddot{\theta}_x + \left[I_b \frac{R}{r^2} \right] \ddot{\beta} - \frac{(R+r)}{r^2} B \dot{\theta}_x - mg \sin \theta_x = 0 \quad (4.1)$$

$$\left[\frac{R(R+r)}{r^2} I_b \right] \ddot{\theta}_x + \left[I_s + \frac{R^2}{r^2} I_b \right] \ddot{\beta} - 2R \frac{(R+r)}{r^2} B \dot{\theta}_x = \tau_y \quad (4.2)$$

$$\left[(R+r)m + I_b \frac{(R+r)}{r^2} \right] \ddot{\theta}_y + \left[I_b \frac{R}{r^2} \right] \ddot{\alpha} - \frac{(R+r)}{r^2} B \dot{\theta}_y - mg \sin \theta_y = 0 \quad (4.3)$$

$$\left[\frac{R(R+r)I_b}{r^2} \right] \ddot{\theta}_y + \left[I_s + \frac{R^2}{r^2} I_b \right] \ddot{\alpha} - \frac{2R(R+r)}{r^2} B \dot{\theta}_y = \tau_x \quad (4.4)$$

Where τ_y is the torque exerted in y-axis direction, I_s is the moment of inertia of the sphere, R is the radius of the sphere, r is the radius of the ball and B is the frictional parameter.

Equations (4.1), (4.2), (4.3) and (4.4) show the complete mathematical model of the ball-on-sphere system with double axis actuation (i.e. actuation on the x-and y-axes respectively).

4.3 20-SIM VALIDATION OF BALL-ON-SPHERE SYSTEM MODEL

The 20-Sim graphical interface which is an interactive tool for model entry and model processing was used for the validation of the developed ball-on-sphere system model. The dynamic bond graph model was built and processed using 20-sim to ensure that it is error free.

Figure 4.3 shows the validation of bond graph model of the ball-on-sphere system in 20-Sim graphical user interface.

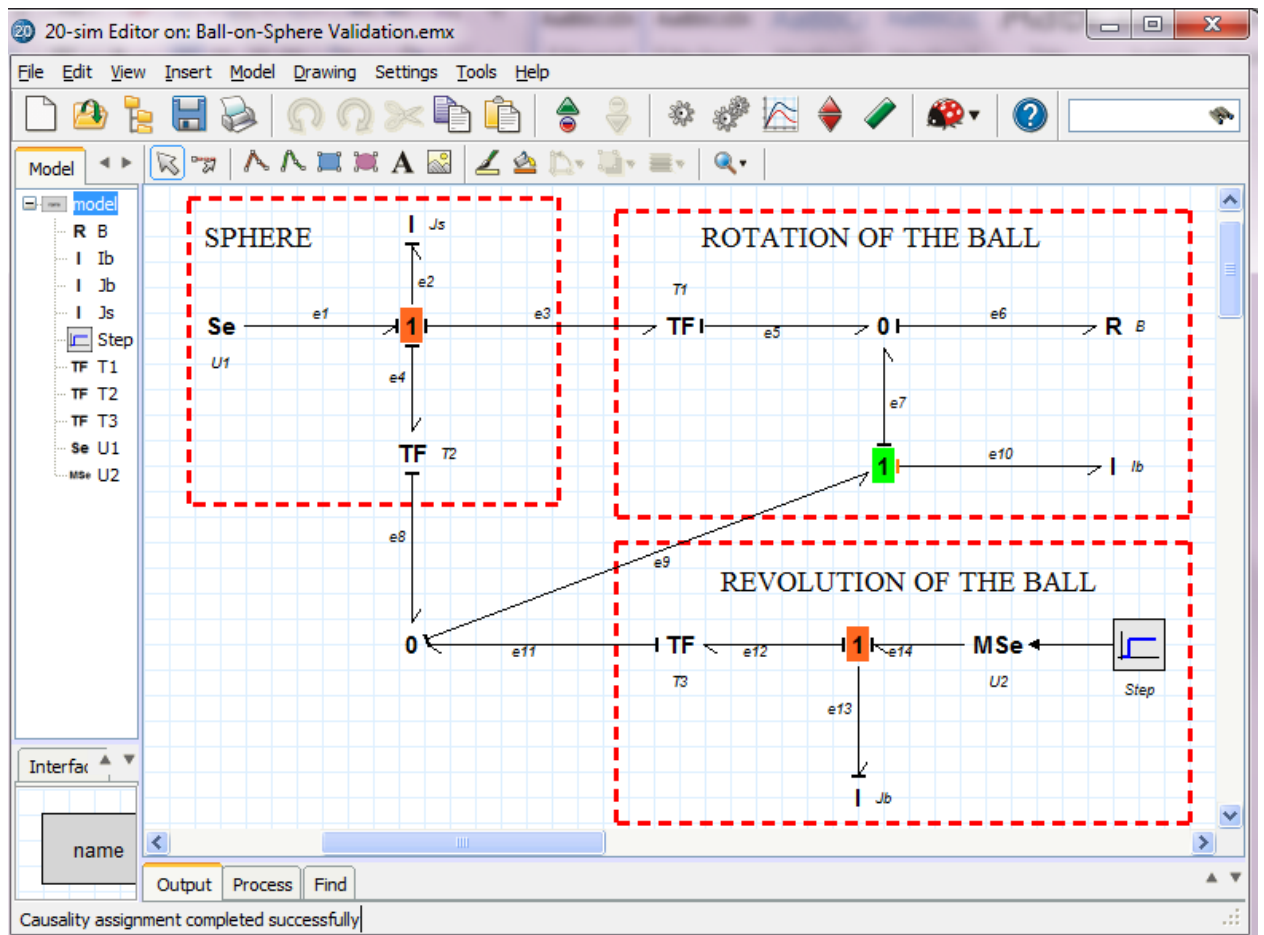


Figure 4.3: Validation of Ball-on-Sphere System using 20-Sim

4.4 STRUCTURAL ANALYSIS OF THE BALL-ON-SPHERE SYSTEM

The results of the structural analysis carried out on the ball-on-sphere system are presented and discuss in following subsections. These include structural controllability, structural observability, inverse model analysis and input-output decoupling analysis of the system.

4.4.1 Ball-on-Sphere System Structural Controllability Analysis

The results of the structural controllability analysis of the ball-on-sphere system are presented in Figure 4.4 and Figure 4.5. The storage elements (I:Js and I:Jb) and the sources of energy (Se and MSe) satisfied the first controllability condition of the system.

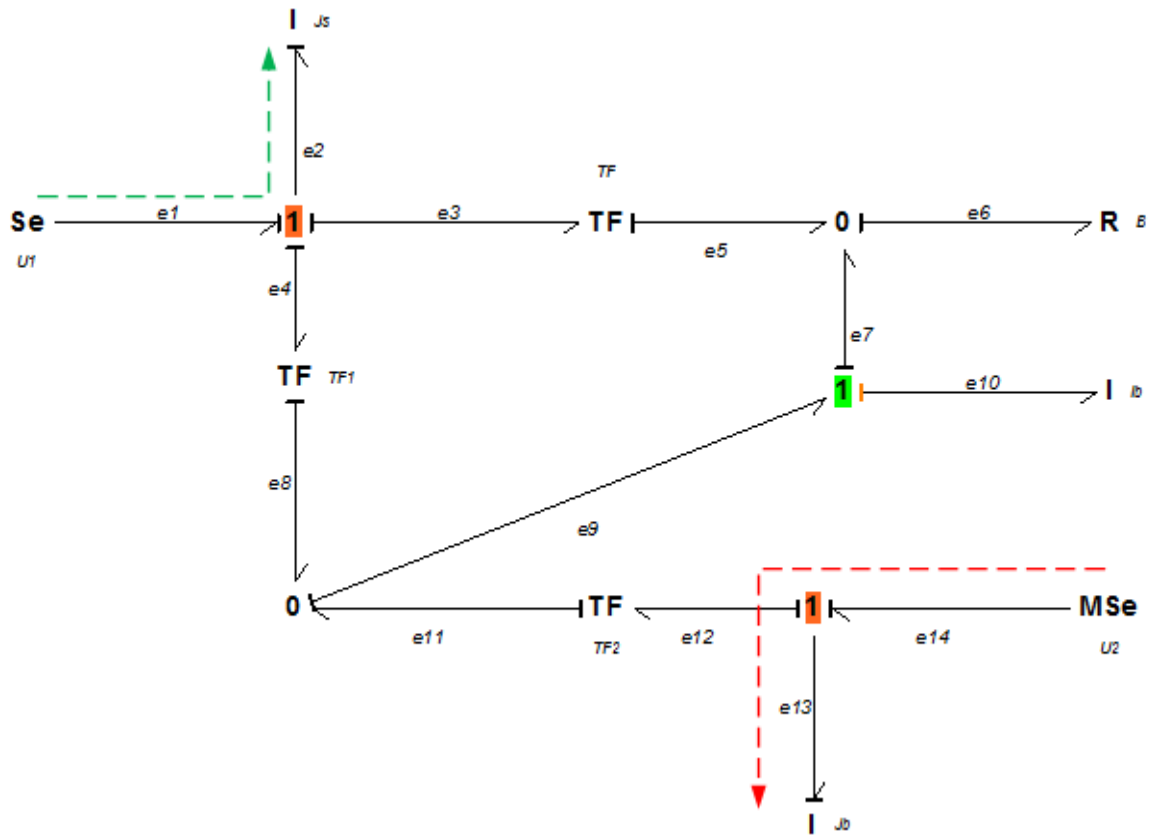


Figure 4.4: Controllability Analysis of the Bond-on-Sphere System Bond Graph Model with Preferential Integral Causality

Furthermore, the second controllability condition of the system was satisfied by transforming the integral storage elements (I:Js and I:Jb) to preferential derivative causalities without violating the system causalities norm.

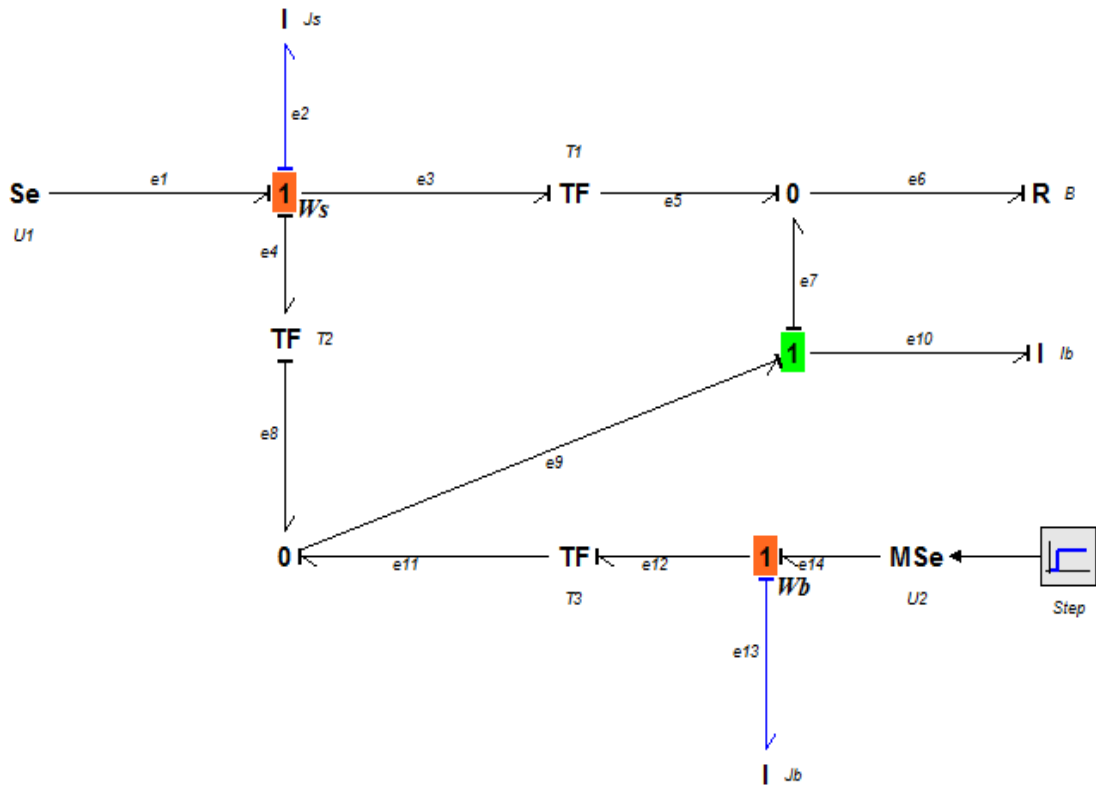


Figure 4.5: Controllability Analysis of the Bond-on-Sphere System Bond Graph Model with Preferential Derivative Causality

Figure 4.4 and Figure 4.5 satisfied the bond graph structural controllability analysis conditions. Hence, the controllability conditions of ball-on-sphere system are satisfied and as such, the ball-on-sphere system is controllable.

4.4.2 Ball-on-Sphere System Structural Observability Analysis

The results of the structural Observability analysis of the ball-on-sphere system are presented in Figure 4.6 and Figure 4.7. The integral storage elements (I:Js and I:Ib) and detectors (Df: Ws and Df: Wb) satisfied the first observability condition of the system.

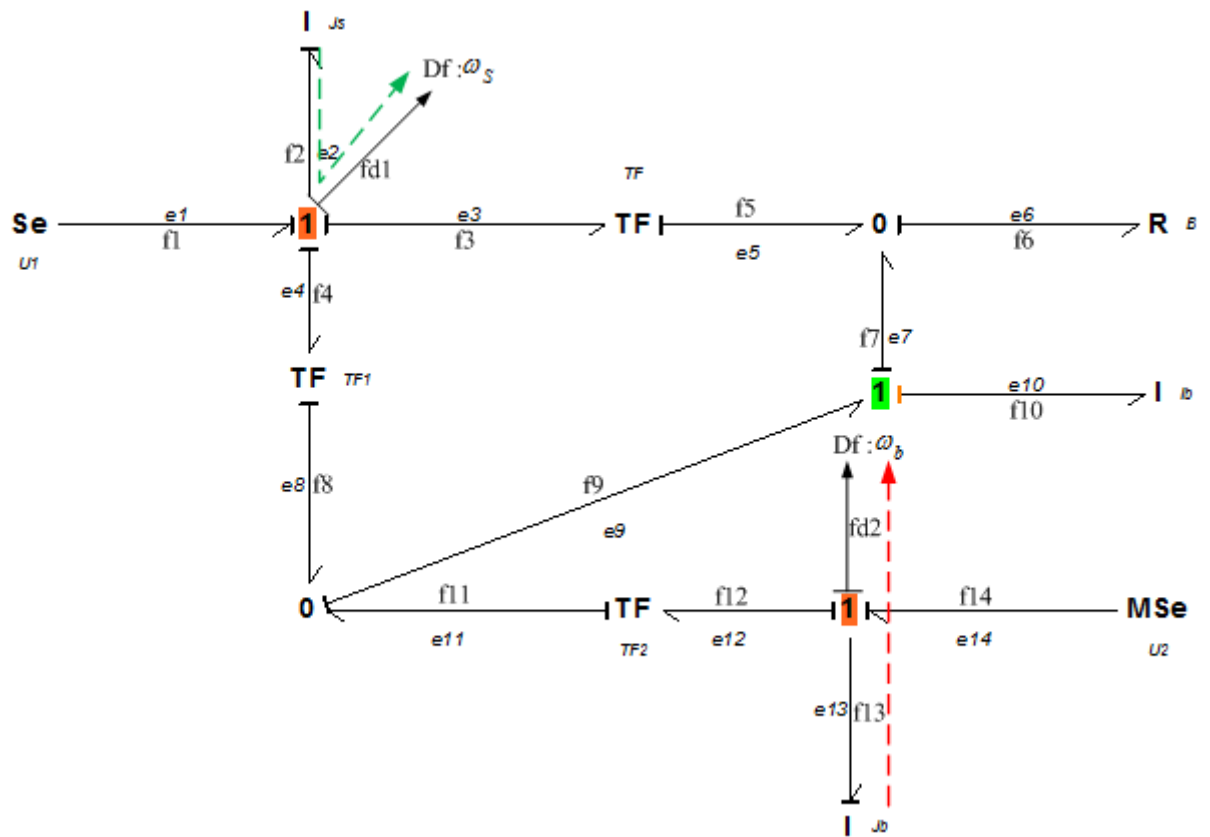


Figure 4.6: Observability Analysis of the Bond-on-Sphere System Bond Graph Model with Preferential Integral Causality

Furthermore, the second observability condition of the system was satisfied by transforming the integral storage elements (I:Js and I:Jb) to preferential derivative causalities without violating the restricted causalities of the system.

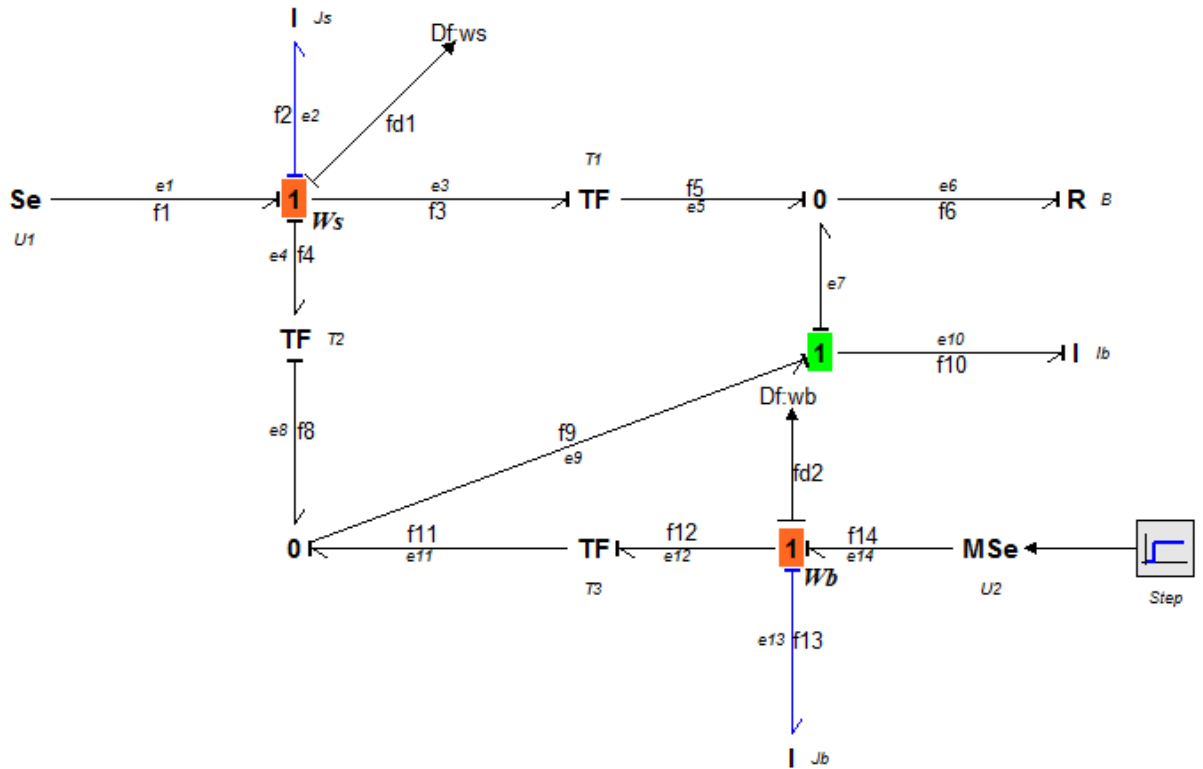


Figure 4.7: Observability Analysis of the Bond-on-Sphere System with Preferential Derivative Causality

From Figure 4.6 and Figure 4.7, the structural observability analysis conditions of the system were satisfied and as such, the ball-on-sphere system is observable.

4.4.3 Ball-on-Sphere System Bond Graph Inverse Model

The result of the bond graph inverse model of the ball-on-sphere is presented in Figure 4.8. Bi-causality assignment procedures were used to obtain the inverse model of the system. The bi-causality allows both conjugate powers into the connected subsystems and propagation was done along the input-output power lines on the ball-on-sphere system model according to the sequential causality assignment procedures for inversion (SCAPI).

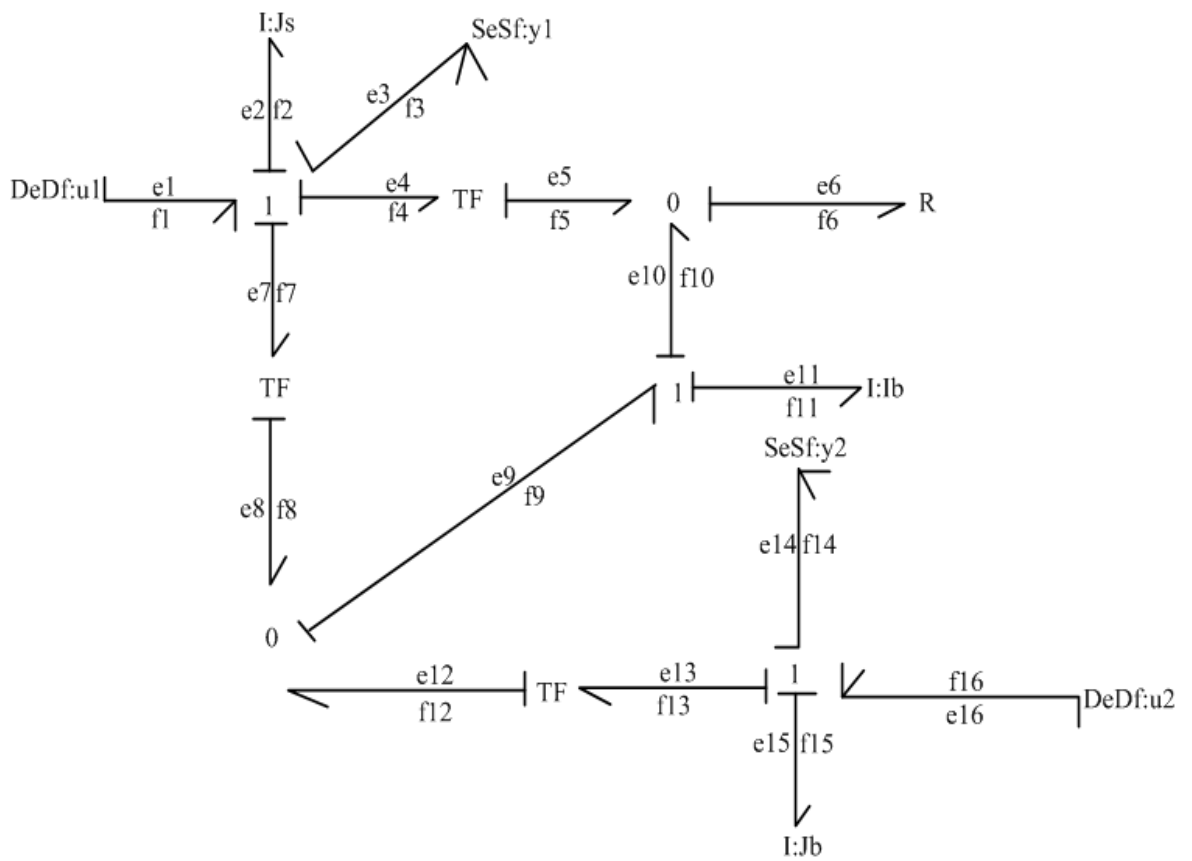


Figure 4.8: Inverse Bond Graph Model of the Ball-on-Sphere System

4.4.4 Ball-on-Sphere System Input-Output Decoupling Analysis

Figure 4.9 was used to analyze the input-output analysis of the ball-on-sphere system bond graph model.

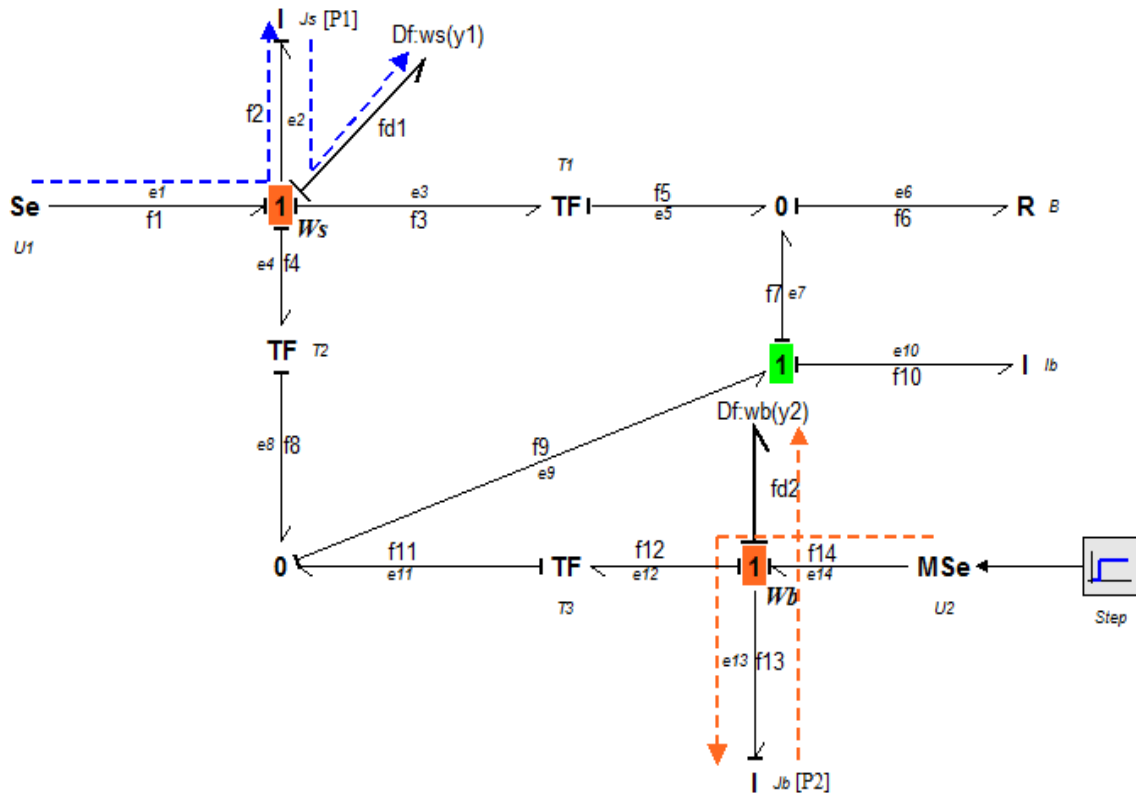


Figure 4.9: Bond-on-Sphere System Model for Decoupling Analysis

From Figure 4.9; the state (x), the input (u) and the output (y) vectors of the ball-on-sphere system are given as:

$$x = [p_1 p_2]^T$$

$$u = [u_1 u_2]^T$$

$$y = [y_1 y_2]^T$$

In the input-output decoupling analysis, the bond-on-Sphere system has two independent input-output power lines: (u_1, y_1) and (u_2, y_2) , thus the ball-on-sphere system is invertible. The disjoint input-output causal paths of the ball-on-sphere system bond graph model are:

$$(u_1, y_1): e_1 - e_2 - f_2 - f_{d1} \text{ and}$$

$$(u_2, y_2): e_{14} - e_{13} - f_{13} - f_{d2}$$

Then, using the length of these causal paths, $L_2 = 2 = 1 + 1$

As such, $l_1 = 1$ and $l_2 = 1$, then $L_2 = l_1 + l_2$ and the ball-on-sphere system is decouplable.

Where l_i is the length of the causal path which is the number of storage elements in the bond graph preferential integral causality met between an output y_i and an input u_i . L_2 is the total number of the causal paths in the bond graph model.

4.5 NUMERICAL APPROACH TO THE BALL-ON-SPHERE SYSTEM ANALYSES

The controllability and observability test was carried out using the Kalman numerical matrix approach to verify whether control solution exist for the ball-on-sphere system.

The ball-on-sphere system is said to be controllable and observable if it is of full rank.

The Matlab script for the controllability and observability tests are as follows:

%Determining the Controllability and Observability of the Ball and Sphere System

Mcr=ctrb(A,B);

Mob=obsv(A,C);

if rank(Mcr)==size(A)

'System is Controllable'

else

'System is NOT Controllable'

end

CONTR_RANK=rank(Mcr)

if rank(Mob)==size(A)

'System is Observable'

else

'System is NOT Observable'

end

OBSV_RANK=rank(Mob)

[Q,R]=optqr(A,B);

ans =

The ball-on-sphere system is controllable

CONTR_RANK = 8

ans =

The ball-on-sphere system is Observable

OBSV_RANK = 8

The complete code for determining the controllability and observability of the ball-on-system system can be found in Appendix A.

The ball-on-sphere system is state controllable and observable from the Kalman matrix numerical analysis approach. Similarly, the ball-on-sphere system is invertible and input-output decouplable from the numerical matrix algebraic approach as presented in section 3.7.

Thus, comparing with the conventional matrix numerical approach, the effectiveness of bond graph based structural analysis approach is verified. The bond graph approach does not depend on parameters of state matrices A and B and it efficiently overcame the complex computation of the conventional numerical matrix approach.

4.6 RESULTS OF BALL-ON-SPHERE MODEL ANALYSIS

The developed ball-on-sphere system model was simulated and analyzed using Linear Quadratic Regulator (LQR) controller. Figure 4.10 shows the comparison of the simulated results of the developed ball-on-sphere system model with effect of friction and without frictional effect in the model. From the simulated parameters, the time of angular position response of the ball (β) achieved with the model with friction was 0.5253s. While in the model without friction consideration, time of 0.5408s for the angular position response of the ball (β) was achieved.

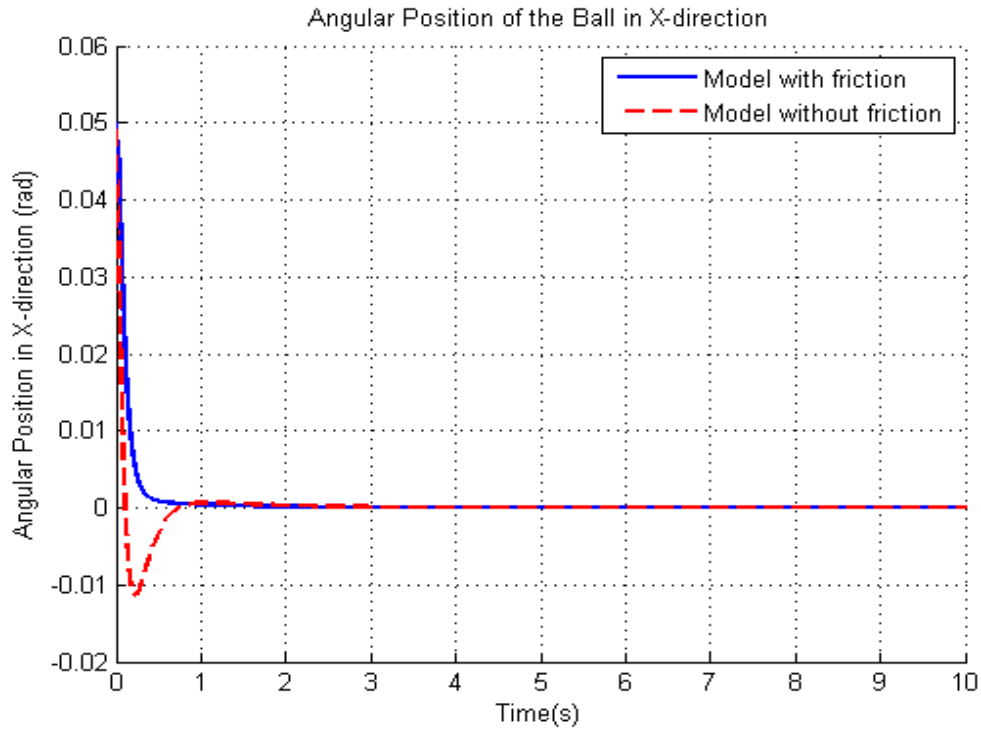


Figure 4.10: Result of Ball-on-Sphere Model Analysis using LQR Controller

Table 4.1 shows comparison of the characteristics of transient response of the ball-on-sphere system model with friction and without frictional effect.

Table 4.1: Comparison of Ball-on-Sphere System Model Results With and Without Friction

The System Response	Model With Friction	Model Without Friction
Rise Time	0.1743	0.1835
Settling Time	0.5253	0.5408
Settling Min	-0.0022	-0.0015
Settling Max	0.0070	0.0050
Overshoot	6.2690e+07	6.3737e+07
Undershoot	1.9450e+06	1.9318e+06
Peak	0.0701	0.0500
Peak Time	0.0026	0.0018

The Matlab codes used for the ball-on-sphere system model with and without friction can be found in appendix B.

CHAPTER FIVE

CONCLUSION AND RECOMMENDATION

5.1 SUMMARY

This research has proposed modelling and structural analysis of the ball-on-sphere system using bond graph technique. The technique is an efficient and simplified approach of modeling the ball-on-sphere system in order to reduce the complexity of the Euler-Lagrange modeling approach which is prone to modelling error. Also, the bond graph technique was used to carry out structural analysis of the developed model in order to evaluate the dynamic behaviour of the system. The whole dissertation is summarized in this chapter. Conclusion, recommendation and limitation of the research work are presented. Areas of future research have also been suggested.

5.2 CONCLUSION

The ball-on-sphere system was modelled using bond graph technique. The technique was used to capture the real dynamic insight of the system in order to address the complexities of the existing technique which is prone to modelling errors due its computational complexities. The 20-Sim software was used to validate the developed model in order to ensure that its error free and the developed mathematical model of the ball-on-sphere were translated into Simulink model. Comparison was made between the developed model with friction and without frictional effect. The results show 2.9% improvement on the angular position response of the ball in the developed bond graph model with frictional effect. Furthermore, bond graph technique was also used to carry out structural analysis of the information properties of the ball-on-sphere system in order to study the dynamic behaviour of the system.

5.3 LIMITATIONS

- 1) The physical experiment test bed of the ball-on-sphere system was not yet in place. This would have contributed to the understanding of the dynamic behaviour of the system.
- 2) In the developed bond graph model of the ball-on-sphere system, the gyrator (GY) element was not considered. This would have contributed to the better understanding of the different domains in the system.

5.4 SIGNIFICANT CONTRIBUTIONS

Several research works have been carried out on the modelling of the ball-on-sphere system using Euler-Lagrange technique. However, the technique is prone to modelling errors due to its computational complexities and is also limited in its capacity to carry out structural analysis of the system.

The significant contributions of this research work are as follows:

- 1) Development of a bond graph based model of the ball on sphere system which is simpler and more efficient for its structural analysis.
- 2) In the developed bond graph model with effect of friction, the time of angular position response of the ball (β) achieved was 0.5253s while in the bond graph model without frictional effect, time of 0.5408s was achieved for the angular position response of the ball (β). This shows 2.9% improvement on the angular position response of the ball considering frictional effect in the developed bond graph model.

5.5 RECOMMENDATIONS FOR FURTHER WORK

The following possible areas of further work are recommended for consideration for future research:

- 1) The developed causal bond graph model can be used to simplify stability study of the ball-on-sphere system.
- 2) An experimental test bed can be carried out to study the dynamic behaviour of the system.
- 3) The bond graph modeling approach can be extended to multi-domain systems.

REFERENCES

- Alabakhshizadeh, A., Iskandarani, Y., Hovland, G. & Midtgård, O. M. (2011). Analysis, modelling and simulation of mechatronic systems using the bond graph method. *Modelling, Identification and Control*, 32, 35-45.
- Alireza, M. S., Ehsan, Z., Yousef, B.-L. & Mohammad, T. (2014). Control of a ball on sphere system with adaptive neural network method for regulation purpose. *Journal of Applied Sciences*, 14(17), 2014.
- An, C. H., Atkeson, C. G. & Hollerbach, J. M. (1988). Model-based control of a robot manipulator: *MIT press Cambridge, MA*, Vol. 214.
- Bambagini, M. & Di Natale, M. (2012). Ball and Plate Model. In ReTiS Lab, Ecole Superior St. Ann, Pisa, Italy.
- Benmoussa, S., Bouamama, B. O. & Merzouki, R. (2014). Bond graph approach for plant fault detection and isolation: Application to intelligent autonomous vehicle. *IEEE Transactions on Automation Science and Engineering*, 11(2), 585-593.
- Bertrand, J.-M. (1997). Structural analysis and input-output decoupling control of bond-graph models. (Doctoral dissertation, University of Lille), *Institute for Scientific and Technical Information*.
- Binder, E. M., Hirokawa, N. & Windhorst, U. (2009). Nonlinear Control Systems. *Encyclopedia of Neuroscience*, 1-9.
- Bobaşu, E., Roman, M. & Şendrescu, D. (2010). Bond Graph Modelling and Nonlinear Control of an Inverted Pendulum. *In Process Control 2010* (1), 1-5.
- Borutzky, W. (2011). Bond graph modelling of engineering systems. *New York: Springer*, (pp. 4-10).
- Borutzky, W., Orsoni, A. & Zobel, R. (2006). Bond graph modelling and simulation of mechatronic systems an introduction into the methodology. *Proceedings of the 20th European Conference on Modelling and Simulation (ECMS)*, Bonn, 2006.
- Broenink, J. F. (1999). 20-sim software for hierarchical bond-graph/block-diagram models. *Simulation Practice and Theory*, 7(5), 481-492.
- Burns, R. (2001). Advanced control engineering: *Butterworth-Heinemann*.
- Chikhaoui, Z., Gomand, J., Malburet, F., Pavel, M., & Barre, P. J. (2013, May). Towards an energetic modeling of rotorcraft using Bond-Graphs. In *American Helicopter Society (AHS) International Forum 69* Vol. 1, No. 1, (pp. 1-17).
- Craig, J. J. (2005). Introduction to robotics: *mechanics and control*. Upper Saddle River: Pearson Prentice Hall, Vol. 3, (pp. 48-70).

- Dauphin-Tanguy, G., Rahmani, A. & Sueur, C. (1999). Bond graph aided design of controlled systems. *Simulation Practice and Theory*, 7(5), 493-513.
- Deur, J., Ivanović, V., Assadian, F., Kuang, M., Tseng, E. H., & Hrovat, D. (2012). Bond graph modelling of automotive transmissions and drivelines. *IFAC Proceedings Volumes*, 45(2), 427-432.
- Falb, P. L., & Wolovich, W. A. (1967). On the decoupling of multivariable systems. *In Joint Automatic Control Conference* (No. 5, pp. 791-796).
- Galindo, R., Gonzalez, G., & Juarez, R. I. (2006). Structural controllability and observability in closed loop for LTI stable systems. In *Computer Aided Control System Design, 2006 IEEE International Conference on Control Applications, 2006 IEEE International Symposium on Intelligent Control, 2006 IEEE* (pp. 2623-2628).
- Gawthrop. (1994). Bicausal bond graphs. *simulation series*, 27, 83-83.
- Gawthrop. (1998). Physical interpretation of inverse dynamics using bond graphs. *The Bond Graph Digest*, 2(1), 23pp.
- Graf, C. & Röfer, T. (2010). A closed-loop 3D-LIPM gait for the RoboCup Standard Platform League humanoid. *Proceedings of the Fifth Workshop on Humanoid Soccer Robots*, Bremen, Germany 2010.
- Hassan. (2003). *Nonlinear Systems Third Edition*, Prentice Hall, 750, ISBN 0-13-067389-7. 47(4), 208.
- Henson, M. A. & Seborg, D. E. (1991). Critique of exact linearization strategies for process control. *Journal of Process Control*, 1(3), 122-139.
- Ho, M.-T., Rizal, Y. & Cheng, W.-S. (2013). Stabilization of a vision-based ball-on-sphere system. *IEEE International Conference on Control Applications (CCA)*, 2013. (pp. 929-934).
- Ho, M.-T., Tu, Y.-W. & Lin, H.-S. (2009). Controlling a ball and wheel system using full-state-feedback linearization [Focus on Education]. *Control Systems, IEEE*, 29(5), 93-101.
- Kailath, T. (1980). *Linear systems: Prentice-Hall Englewood Cliffs, NJ*, (Vol. 1).
- Karim, A., Sueur, C. & Dauphin-Tanguy, G. (2003). Non-regular static state feedback for linear bond graph models. *Proceedings of the Institution of Mechanical Engineers, Part I: Journal of Systems and Control Engineering*, 217(2), 61-71.
- Karnopp, D. C., Margolis, D. L. & Rosenberg, R. C. (2012). Multiport Systems and Bond Graphs. *System Dynamics: Modelling, Simulation, and Control of Mechatronic Systems, Fifth Edition*, 17-36.
- Kayani, S. A. & Malik, M. A. (2008). Bond-graphs+ genetic programming: Analysis of an automatically synthesized rotary mechanical system. In *Proceedings of the 10th*

- Annual Conference Companion on Genetic and Evolutionary Computation*. (pp. 2165-2168).
- Lane, S. H., & Stengel, R. F. (1988). Flight control design using non-linear inverse dynamics. *Automatica*, 24(4), 471-483.
- Ledin, J. (2001). *Simulation engineering*: CMP books The Netherlands.
- Lee, P. & Sullivan, G. (1988). Generic model control (GMC). *Computers & chemical engineering*, 12(6), 573-580.
- Liu, S. Y., Rizal, Y., & Ho, M. T. (2011). Stabilization of a ball and sphere system using feedback linearization and sliding mode control. In *8th Asian Control Conference (ASCC), 2011* (pp. 1334-1339).
- Mahindrakar, A. & Kulkarni, S. (2012). Bond graph analysis of the engineering systems using 20-sim software tool. *International journal of engineering science & advanced technology*, 2(5), 1431-1434.
- Matsuda, Y., & Ohse, N. (2006). Synthesis of dynamic controllers for a class of nonlinear systems: An application to a ball-on-wheel system. In *Computer Aided Control System Design, 2006 IEEE International Conference on Control Applications, 2006 IEEE International Symposium on Intelligent Control*, (pp. 1061-1066).
- Moezi, S. A., Zakeri, E. & Bazargan-Lari, Y. (2014). Control of a ball on sphere system with adaptive neural network method for regulation purpose. *Journal of Applied Sciences*, 14(17), 2014.
- Moezi, S. A., Zakeri, E., Bazargan-Lari, Y. & Khalghollah, M. (2014). Fuzzy Logic Control of a Ball on Sphere System. *Advances in Fuzzy Systems*, 2014.
- Mohammad, N. & Khashabi, D. (2011). Modelling and Control of Ball and Plate System. *Amirkabir University of Technology*, 1-22.
- Morari, M. & Zafiriou, E. (1989). *Robust process control*: PTR Prentice Hall, New Jersey.
- Ngwompo, R., Scavarda, S. & Thomasset, D. (1997). Structural Invertibility and Minimal Inversion of Multivariable Linear Systems-A Bond Graph Approach. *simulation series*, 29, 109-114.
- Ngwompo, R. F. (2011). Bond graph-based filtered inversion of multivariable physical systems. *Proceedings of the Institution of Mechanical Engineers, Part I: Journal of Systems and Control Engineering*, 226(1), 125-140.
- Orlikowski, C. & Hein, R. (2011). Modelling and analysis of beam/bar structure by application of bond graphs. *Journal of Theoretical and Applied Mechanics*, 49(4), 1003-1017.

- Paynter, H. (1970). System graphing concepts. *Instruments & control systems*, 43(7), 77.
- Porter, W. A. (1969). Decoupling of and inverses for time-varying linear systems. *IEEE Transactions on Automatic Control*, 14(4), 378-380.
- Rahmani, A., Sueur, C., & Dauphin-Tanguy, G. (1996). On the infinite structure of systems modelled by bond graph: feedback decoupling. *IEEE International Conference on Systems, Man, and Cybernetics, 1996*. (Vol. 3, pp. 1617-1622).
- Margetts, R. (2013). Modelling & analysis of hybrid dynamic systems using a bond graph approach. (*Doctoral dissertation, University of Bath*).
- Sharon, A., Hogan, N. & Hardt, D. E. (1991). Controller design in the physical domain. *Journal of the Franklin Institute*, 328(5), 697-721.
- Sueur, C. & Dauphin-Tanguy, G. (1989). Structural controllability/observability of linear systems represented by bond graphs. *Journal of the Franklin Institute*, 326(6), 869-883.
- Sueur, C. & Dauphin-Tanguy, G. (1991). Bond-graph approach for structural analysis of MIMO linear systems. *Journal of the Franklin Institute*, 328(1), 55-70.
- Willson, S. S., Daly, K., Mullhaupt, P. & Bonvin, D. (2012). Quotient method for stabilising a ball-on-a-wheel system—Experimental results. *IEEE 51st Annual Conference on Decision and Control (CDC)*, 2012. (pp. 1271-1278).
- Yu, B. & Van Paassen, A. (2004). Simulink and bond graph modeling of an air-conditioned room. *Simulation Modelling Practice and Theory*, 12(1), 61-76.
- Zakeri, E., Ghahramani, A., Moezi, S. A. & Yousef Bazargan-Lari. (2012). Adaptive Feedback Linearization Control Of a Ball on Sphere System. *International Conference on Mechanical Engineering and Advanced Technology*.

APPENDIX A

BALL-ON-SPHERE SYSTEM CONTROLLABILITY AND OBSERVABILITY ANALYSIS

```
close all
clc
%Parameter definition of the ball-on-sphere system
function [m,r,R,Ib,IB,g,Ra,d,Kb]=paramBandP
m=0.012;      %kg
r=0.011;     %m
R=0.099;     %m
Ib=5.808e-7; %kg.m_sq
IB=0.99;     %kg.m_sq
g=9.8;      %m/s_sq
Ra=0.6510;  %Ohms
d=0.032;    %m
Kb=0.0643;  %N-m/A

function [X2,X3,X4,X5,X1,X6,X7,X8,t,x,A,B,C,D]=stateparamBandP
%%%%%%%%%%%%%%%%%%%%%%%%%%%%%%%%%%%%%%%%%%%%%%%%%%%%%%%%%%%%%%%%%%%%%%%%
psi=0.05;
%' psi' must be less than or equal to 0.4
[m,r,R,Ib,IB,g,Ra,d,Kb]=paramBandP;
Is=IB;
b1=R*Kb/d/Ra;
b2=-Ra*b1^2;
B=psi*b2*(-(r^2)/(2*(R*(R+r))));
a1=m*(R+r)+Ib*(R+r)/r^2;
a2=Ib*R/r^2;
a3=-(R+r)*B/r^2;
a4=-m*g;
a5=Ib*R*(R+r)/r^2;
a6=Is+R^2/r^2*Ib;
a7=-2*R*(R+r)*B/r^2;

M11=[1 0 0 0 ;0 a1 0 a2; 0 0 1 0; 0 a5 0 a6];

M12=zeros(size(M11));

M=[M11 M12; M12 M11];

A11=[0 1 0 0 ;-a4 -a3 0 0; 0 0 0 1; 0 -a7+b2 0 0];

A12=zeros(size(A11));

A=[A11 A12 ; A12 A11];

B11=[0 ;0; 0; b1];

B12=zeros (size(B11));
```

```

B= [B11 B12 ; B12 B11];
C=eye(size(A));
D=0;
A=(M^-1)*A;
B=(M^-1)*B;
[Q,R]=optqr(A,B);

[X2,X3,X4,X5,X1,X6,X7,X8,t,x,A,B,C,D]=stateparamBandP;
%MATLAB M-FILE for Controllability and Observability Analysis of the %Ball and
Sphere System
Mcr=ctrb(A,B);
Mob=obsv(A,C);
if rank(Mcr)==size(A)
'System is Controllable'
else
'System is NOT Controllable'
end
CONTR_RANK=rank(Mcr)
if rank(Mob)==size(A)
'System is Observable'
else
'System is NOT Observable'
end
OBSV_RANK=rank(Mob)

```

APPENDIX B

BALL-ON-SPHERE MODEL ANALYSIS

```
close all
clc
psi=0.05;
[m,r,R,Ib,IB,g,Ra,d,Kb]=paramBandP;
Is=IB;
b1=R*Kb/d/Ra;
b2=-Ra*b1^2;
B=psi*b2*(-(r^2)/(2*(R*(R+r)))));
a1=m*(R+r)+Ib*(R+r)/r^2;
a2=Ib*R/r^2;
a3=-(R+r)*B/r^2;
a4=-m*g;
a5=Ib*R*(R+r)/r^2;
a6=Is+R^2/r^2*Ib;
a7=-2*R*(R+r)*B/r^2;
M11=[1 0 0 0; 0 a1 0 a2; 0 0 1 0; 0 a5 0 a6];
M12=zeros(size(M11));
M=[M11 M12 M12 M11];
A11=[0 1 0 0; -a4 -a3 0 0; 0 0 0 1; 0 -a7+b2 0 0];
A12=zeros(size(A11));
A=[A11 A12; A12 A11];
B11=[0 0 0 b1];
B12=zeros(size(B11));
B=[B11 B12 ; B12 B11];
C=eye(size(A));
D=0;
%
[m,r,R,Ib,IB,g,Ra,d,Kb]=paramBandP;
function [X2,t,x,A,B,C,D]=stateparamBandPwithFriction
a1=(R+r)*m +Ib*(R+r)/r^2;
a2=Ib*R/r^2;
a3=-m*g;
a4=Ib*R*(R+r)/r^2;
a5=IB+Ib*(R/r)^2;
M11=[1 0 0 0; 0 a1 0 a2; 0 0 1 0 ;0 a4 0 a3];
M12=zeros(size(M11));
M=[M11 M12; M12 M11];
A11=[0 1 0 0 ;-a3 0 0 0 ;0 0 0 1; 0 0 0 0];
%
A12=zeros(size(A11));
A=[A11 A12; A12 A11];
```

```

B11=[0 0 0 1];
B12=zeros(size(B11));
B=[B11 B12 ; B12 B11];
C=eye(size(A));
D=0;
% designing LQR controller settings
A=(M^-1)*A;
B=(M^-1)*B;
[Q,R]=optqr(A,B);
[K ~,~]=lqr(A,B,Q,R);% Q and R
%
[K P E]=lqr(A,B,Q,R);% Q and R
%
sys_LQ=ss(A-B*K,B,C,D);
%
pzmap(sys_LQ)
%
sgrid
%pause
x=[0.05 0.02 0 0 0.07 0.05 0 0];
t=0:0.0002:10;
%
sgrid
%pause
%
x0=initial(sys_LQ,x,t);
X2=[1 0 0 0 0 0 0 0]*x0';
function BonS
close all
clc
[X2,t,x,A,B,C,D]=stateparamBandPwithfriction ;
[X2b,tb,xb,Ab,Bb,Cb,Db]=stateparamBandPNoFriction;
plot(t,X2,'b')
plot(tb,X2b,'r')
ylabel('Angular Position in X-direction (rad)')
title('Angular Position of the Ball in X-direction')
legend({'Model with friction','Model without friction'})
grid on
%Matlab code for computing the transfer function matrix
sys=ss(A,B,C,D);
tf(sys)

```